Numerical Results for Flows and Heat Transfer Due to Nonlinearly and Exponentially Stretching Surfaces with Variable Fluid Properties

Razia Sharif

Thesis submitted for the degree of

Master of Philosophy in Mathematics

Supervisor: Dr. Muhammad Asif Farooq

School of Natural Sciences(SNS)

National University of Sciences and Technology(NUST)

Islamabad, Pakistan

FORM TH-4

National University of Sciences & Technology

MS THESIS WORK

We hereby recommend that the dissertation prepared under our supervision by: Ms. Razia Sharif, Regn No. 00000172993 Titled Numerical Results for Flows and Heat Transfer Due to Nonlinearly and Exponentially Stretching Surfaces with Variable Fluid Properties be accepted in partial fulfillment of the requirements for the award of **MS** degree.

Examination Committee Members

1. Name: DR. MUJEEB UR REHMAN Signature: _____

2. Name: DR. MERAJ MUSTAFA HASHMI Signature: _____

External Examiner: PROF. MUHAMMAD AYUB Signature: _____

Supervisor's Name DR. M. ASIF FAROOQ Signature: _____

_____ 16/08/18
Head of Department Date

COUNTERSINGED

Date: 16/08/18

Dean/Principal

THESIS ACCEPTANCE CERTIFICATE

Certified that final copy of MS thesis written by **Ms. Razia Sharif** (Registration No. **00000172993**), of **School of Natural Sciences** has been vetted by undersigned, found complete in all respects as per NUST statutes/regulations, is free of plagiarism, errors, and mistakes and is accepted as partial fulfillment for award of MS/M.Phil degree. It is further certified that necessary amendments as pointed out by GEC members and external examiner of the scholar have also been incorporated in the said thesis.

Signature: _____

Name of Supervisor: Dr. M. Asif Farooq

Date: 16/08/2018

Signature (HoD): _____

Date: 16 Aug, 2018

Signature (Dean/Principal): _____

Date: 16/08/18

Dedicated to

my Mother who taught me to trust Allah

and believe in hardwork

and to my great father

who always encourage and support me.

Acknowledgement

I am grateful to my supervisor, ***Dr. Muhammad Asif Farooq*** whose generous guidance and support made it possible for me to work on a topic that was of great interest to me. It was a pleasure working with him.

I would like to thank my seniour ***Laraib Hanif*** and ***Naila Mehreen*** for their guidance throughout my MS. Thanks to my friends for giving the right advice at the right time and for being a source of motivation.

Abstarct

The main motivation behind this work has been to observe the impact of variable fluid properties on flow and heat transfer occuring due to non-linearly and exponentially stretching surfaces. It can happen that the fluid properties change significantly if the temperature difference rises. The result of this temperature difference on fluid flow is that dynamical and thermodynamical properties cannot remain constant. Therefore, thermal analysis with variable properties is required for correct interpretation of results.

The governing physical model is very simple i.e. Navier-Stokes equations have been the underlying model with 2D, laminar, viscous and incompressilbe flows. Boundary layer assumption make-up the governing equation even further simpler.

Nonlinearity of the governing equation as well as coupling of the system make it difficult to find solutions. Due to this limitation we apply numerical methods to solve coupled ODEs which have been obtained by applying similarity transformation to the PDEs.

Post processing of the solutions has been completed by constructing tables and presenting figures against different physical parameters.

We observe a significantly different behaviour of velocity and temperature profiles when variable viscosity have been compared with constant fluid properties.

Contents

Chapter 1

Introduction

Fluid mechanics is the branch of mechanics which deals with gases and liquids which are either at rest or in motion. Applications of fluid mechanics are enormous e.g breathing, swimming, blood flow, airplanes, missiles, pumps, fans, turbines, ships, rivers, windmills, pipes and filters etc.
This chapter is classified as follows: Section 1.1, consist of literature review. Section 1.2, contains some important definitions. In Section 1.3, numerical methods are explained in detail.

1.1 Literature Review

Blasius [1] was the first person who made formal attempt towards understanding boundary-layer theory. He consider a 2D, steady boundary layer flow over a flate plate. In 1961 Sakiadis [2, 3, 4] in a series of papers discussed the flow analysis for axisymmetric, continuous flat surface and continuous cylindrical surface. Soundalgekar et. al [5] discussed the heat transfer analysis of the flow due to a continuous moving plate while keeping the temperature as variable. Andersson and Aarsaeth [7] revisited the problem of Sakiadis flow for variable fluid properties. The MHD heat

transfer analysis in the case of non-isothermal sheet has been examined by Chiam [10]. Mukhopadhyay et al. [11] in their work taken a heated surface while the flow is MHD and the varying viscosity. In a series of papers Pop et al. [12] and Prasad et al. [13] examined the effect of variable viscosity over a continuous surfaces. MHD viscoelastic flow past a stretching sheet with transverse magnetic field presented in Andersson [15]. Mabood et al. [33] developed an analytical solution for viscous incompressible flow over a sheet that stretched exponentially.

1.2 Basic Definitions and Preliminaries

1.2.1 Fluid

Fluid is a subtance that deforms continuosly under the action of shearing forces. The fluids are divided into two categories namely, liquids and the gases. Fluids do not have definite shape.

1.2.2 Shear Stress

Shear stress is the tangential force per unit area. Mathematically we write

$$\tau = \frac{F}{A},$$

here τ denotes the shear stress, F is stands for applied force and A is area. The wall shear stress is defined as

$$\tau_w = \mu \left(\frac{\partial u}{\partial y} \right)_{y=0}.$$

1.2.3 Newtons Law of Viscosity

Viscosity is a property of the fluid which opposes the relative motion between the two layers of the fluid that are moving at different velocities. It is temperature

dependent: In liquids it decreases with increase in temperature while for gases it shows opposite behaviour. The relation between shear stress and shear strain rate is defined by Newton's law. Mathematically we write

$$\tau = \mu \frac{du}{dy}.$$

1.2.4 Density

The density is mass per unit volume. It is expressed mathematically as

$$\rho = \frac{m}{V}.$$

The unit of ρ is kg/m^3.

1.2.5 Kinematic Viscosity

A parameter oftenly appear in equation of motionn is kinematic viscosity which is obtained by dividing dynamic viscosity to density of the fluid. Mathematically we write

$$\nu = \frac{\mu}{\rho}.$$

The unit of ν is m^2/sec.

1.2.6 Heat Flux

The heat flux is related with temperature gradient by Fourier's law which is written as

$$\mathbf{q} = -k\nabla T,$$

where $\mathbf{q}$ is heat flux, k is the thermal conductivity and T is the temperature.

1.2.7 Specific Heat Capacity

Specific heat capacity of a substance is the amount of heat required to raise the temperature of 1 gram of the substance by 1 kelvin (or by 1 C^o). It is the property of material that measures how much heat energy is needed to warm the substance. Non-conductors have higher values of specific heat as compared to conductors. Mathematically

$$C = \frac{q}{m\Delta T},$$

where q shows amount of heat energy gained or lost by a substance, m is mass, C is heat capacity and ΔT is change in temperature. SI unit is $\frac{J}{kgK}$.

1.2.8 Prandtl Number

The Prandtl number Pr a is dimensionless number representing the ratio of kinematic viscosity to the thermal diffusivity. It is given as

$$Pr = \frac{C_p \mu}{k},$$

Thermal diffusivity dominates for small values of Prandtl number whereas for large values viscous diffusivity dominates.

1.2.9 Nusselt Number

The Nusselt number Nu, is the ratio of convective to conductive heat transfer in a fluid over a given length. It is written as

$$Nu = \frac{h.L}{k}.$$

where h is the convective heat transfer coefficient of the flow, L is the characteristic length, k denotes thermal conductivity of the fluid. The effect of conduction and convection is same when Nusselt number is considered to be one.

1.2.10 Skin Friction Coefficient

Skin friction is a resistance which occurs when an object moves in a fluid. The skin friction coefficient C_f is defined as

$$C_f = \frac{\tau_w}{\frac{1}{2}\rho U_\infty^2}.$$

1.2.11 Boundary Layer Flows

A boundary layer is a thin layer that form over a bounding surface when a low-viscosity, fast-moving fluid flows over it. Within this layer, the shear stress changes the fluid's velocity profile such that it is zero near the surface and then asymptotically approaches the free-stream velocity U of the flow for away from the surface. In this thin region the effects of viscosity are important.

1.3 Governing Equations

The continuity equation, the conservation of momentum and the conservation of energy are the fundamental equations in fluid mechanics. Most of the fluid flow and heat transfer problems can be explained mathematically by these three equations.

1.3.1 Equation of Continuity

The mass conservation principle deals with the equation of continuity.

$$\frac{\partial \rho}{\partial t} + \nabla.(\rho \mathbf{V}) = 0, \tag{1.3.1}$$

which is the equation of continuity for a compressible fluid. For steady flow

$$\frac{\partial \rho}{\partial t} = 0. \tag{1.3.2}$$

Then the above Eq. (1.3.1) becomes

$$\nabla.(\rho \mathbf{V}) = 0.$$

This is called a contiuity equation or conservation equation of mass. If density ρ is also constant then we get

$$\nabla.\mathbf{V} = 0.$$

1.3.2 Conservation of Momentum

The conservation of momentum is based on the law of conservation of linear momentum.

$$\rho\left(\frac{d\mathbf{V}}{dt}\right) = -\nabla.\pi + \rho\mathbf{g}, \tag{1.3.3}$$

the surface forces are due to the stresses which are summation of the viscous stresses τ_{ij} plus the hydrostatic pressure on the sides of control surface that comes from the motion of the velocity gradients i.e.

$$\pi_{ij} = -p\delta_{ij} + \tau_{ij},$$

so,

$$\nabla.\pi = -\nabla p + \nabla.\tau.$$

After substituting the above relation in Eq. (1.3.3), we get

$$\rho\frac{d\mathbf{V}}{dt} = \rho\mathbf{g} - \nabla p + \nabla.\tau \tag{1.3.4}$$

1.3.3 Conservation of Energy

According to this law energy can neither be created nor destroyed.
Enery equation is given as:

$$Q - W_{sur} - W_{visc} = \frac{\partial}{\partial t}\left(\int_{CV} e\rho dV\right) + \int_{CS}\left(e + \frac{p}{\rho}\right)\rho(\mathbf{V}.\mathbf{n})dA \tag{1.3.5}$$

where $W_{sur} = 0$ because there can be no infinitesimal shaft protruding into the control volume. The right-hand side for tiny element becomes,

$$Q - W_{visc} = \left(\frac{\partial}{\partial t}(\rho e) + \frac{\partial}{\partial x}(\rho u\xi) + \frac{\partial}{\partial y}(\rho v\xi) + \frac{\partial}{\partial z}(\rho w\xi)\right)dxdydz \tag{1.3.6}$$

where $\xi = e + \frac{p}{\rho}$. Using continuity equation the above Eq. (1.3.6) becomes

$$Q - W_{visc} = \left(\rho\frac{de}{dt} + \mathbf{V}.\nabla p + p\nabla.\mathbf{V}\right) dxdydz \tag{1.3.7}$$

To evaluate Q we use Fourier's law of conduction. Adding the inlet terms and subtracting oulet terms, we get

$$Q = -\left(\frac{\partial}{\partial x}(q_x) + \frac{\partial}{\partial y}(q_y) + \frac{\partial}{\partial z}(q_z)\right) dxdydz = -\nabla.\mathbf{q}dxdydz \tag{1.3.8}$$

Introducing Fourier's law, we have

$$Q = \nabla.(k\nabla T)dxdydz \tag{1.3.9}$$

The net viscous work rate after outlet terms are subtracted from inlet terms, becomes

$$W_{visc} = -\nabla.(\mathbf{V}.\tau_{ij})dxdydz \tag{1.3.10}$$

by substituting (1.3.9) and (1.3.10) into Eq. (1.3.7) and eliminate $\nabla.\tau_{ij}$ by using linear momentum equation, we get the final differential form of energy equation:

$$\rho\frac{du}{dt} + p(\nabla.\mathbf{v}) = \nabla.(k\nabla T) + \phi \tag{1.3.11}$$

where $\phi = \tau_{ij}\frac{\partial u_i}{\partial x_j}$.

1.4 Numerical Methods

Numerical techniques are used to find the numerical approximations to the solutions of nonlinear PDEs. These nonlinear PDEs are first converted to nonlinear ODEs by using similarity transformations. There are various methods for finding the numerical solutions like finite difference method, spectral method, shooting method, bvp4c. Here we discuss shooting and bvp4c(built-in MATLAB solver).

1.4.1 Shooting Method

In numerical analysis, shooting technique is used for finding the solution of BVP by reducing the problem into an IVP. Both linear and nonlinear ODEs can be solved by shooting method. In shooting method the basic algorithm is the supposition of trial value. The solution starts at one end of BVP and shoots to other end with an initial guess until the BC at the other end reaches to its exact value.

Consider the following two point BVP with subject to the BCs that is written in the following form as

$$y'' = f(x, y, y'), \quad y(a) = \alpha, \quad y(b) = \beta, \tag{1.4.1}$$

where (α, β) are unknowns.

The Eq. (1.4.1) is converted into IVP by following procedure:

Consider the IVP

$$y'' = f(x, y, y'), \quad y(a) = \alpha, \quad y'(a) = \lambda. \tag{1.4.2}$$

From Eq. (1.4.2) we have to find λ which gives the value of $y(b) = \beta$. The process of solving the linear and nonlinear shooting method is similar except for few cases. The solution to nonlinear problems is same as linear problem except that the base solution cannot be expressed as a linear combination of each other. Moreover we have an iterative procedure rather than a simple formula for combining the solutions of two IVPs for nonlinear case. For a nonlinear BVP, we have to find the zero of function which represents the error i.e. the amount by which the solution to IVP fails to satisfy the boundary condition at $x = b$. In other words the amount by which $y(b, \lambda)$ misses the target value β. This error is denoted by $F(\lambda)$. It is defined as

$$F(\lambda) = y(b, \lambda) - \beta = 0. \tag{1.4.3}$$

when $y'(a) = \lambda$ has been found then the desired solution is $y(x, \lambda)$. Now to find the zero of the error function we can use two different approaches. One approach is

Newton's method and the other approach is secant method. Here we use Newton's method. First we have to calculate the derivative of the function $F(\lambda)$. To choose the value of λ such that Eq. (1.4.3) holds. Then

$$\lambda = y'(a) = \frac{y(b) - y(a)}{b - a} \tag{1.4.4}$$

$$\lambda = \frac{\beta - \alpha}{b - \alpha} \tag{1.4.5}$$

Newton's method is used to approximate the solution of $y(b, \lambda) - \beta = 0$ and find a next guess λ_{k+1}.

$$\lambda_{k+1} = \lambda_k - \frac{y'(b, \lambda_k) - \beta}{y'(b, \lambda_k)} \tag{1.4.6}$$

1.4.2 bvp4c

To find solution of BVP directly we use bvp4c. To solve BVP an estimate is required while programming in MATLAB. The bvp4c is an efficient solver of BVPs. It is based on collocation and solution starts with initial estimate provided initial mesh points. While in shooting technique, the solution is approximated on the whole interval and considering the BCs all the times. The number of mesh points are require to represent the solution upto the specified accuracy.

Chapter 2

Numerical Comparison of Constant and Variable Fluid Properties for MHD Flow Over a Nonlinearly Stretching Sheet

This work is the review work of Chapter 2 of Shafaq [42]. This chapter focuses on flow and heat transfer analysis over a nonlinearly stretched surface. Comparison has been made between constant and variable viscosities. Three cases i.e constant viscosity, viscosity dependence on inverse linear temperature and viscosity dependence on exponential temperature have been studied. The current work deals with numerical solutions for various values of governing parameters.

The present work is organized as follows. In Section 2.1 we present mathematical model for flow and heat transfer analysis. The special cases for the constant and variable viscosity have been discussed in Section 2.2. The computational procedure is given in Section 2.3. In Section 2.4 we present the graphs and tables and their discussion.

2.1 Mathematical Formulation

Here we investigate a steady, 2D and laminar flow due to a nonlinearly stretching surface. x-axis is taken along the sheet and y-axis is normal to it. B_0 is the strength of magnetic field which is applied in normal direction. The sheet moves with a non-uniform velocity $U(x)$ in positive x-direction. Velocity of the sheet is $U_w(x) = ax^m$, where a is a constant and m is an exponent. Temperature of ambient fluid is taken as constant and is denoted by T_o whereas temperature of sheet is of the form $T_w(x) = T_o + cx^n$, where c and n are positive constants. Reynolds number is taken as small so that induced magnetic field becomes insignificant. The governing equations using above assumptions are given as Andersson and Aarsaeth [7].

$$\partial_x(\rho u) + \partial_y(\rho v) = 0, \tag{2.1.1a}$$

$$\rho(uu_x + vu_y) = \partial_y(\mu u_y) - \sigma B_0^2 u, \tag{2.1.1b}$$

$$\rho C_p(uT_x + vT_y) = \partial_y(kT_y), \tag{2.1.1c}$$

and BCs are given by

$$u(x,0) = U_w(x) = ax^m, \quad v(x,0) = 0, \quad T(x,0) = T_w(x) \tag{2.1.2}$$
$$u \to 0, \quad T \to T_0, \quad as\ y \to \infty.$$

where u and v are the x and y-components of velocities repectively. The fluid density is represented by ρ, B_0 shows the strength of the applied magnetic field, dynamic viscosity of the fluid is μ, specific heat is denoted by C_p, temperature of the fluid is T and k denotes thermal conductivity. U_w represents the sheet's velocity, wall temperature is denoted by T_w.

Introducing the following similarity variables Ali [23], Andersson and Aarsaeth [7].

$$\eta = \sqrt{\frac{(1+m)U(x)}{2\nu_0 x}} \int_0^y \frac{\rho}{\rho_0} dy, \qquad \psi = \rho_0 \sqrt{\frac{2\nu_0 x U(x)}{1+m}} f(\eta), \qquad \theta(\eta) = \frac{T - T_0}{T_w - T_0}, \tag{2.1.3}$$

stream function is denoted by ψ and given as

$$\rho u = \frac{\partial \psi}{\partial y}, \qquad \rho v = -\frac{\partial \psi}{\partial x}. \tag{2.1.4}$$

Using Eq. (2.1.4) the x and y components of velocity can be written as

$$u = ax^m f'(\eta), \qquad v = -\rho_0 \sqrt{\frac{2\nu_0 a}{1+m}} x^{\frac{m-1}{2}} \left(\frac{m+1}{2} f(\eta) + \eta \frac{m-1}{2} f'(\eta)\right). \tag{2.1.5}$$

Plug in Eqs. (2.1.3), (2.1.4) and (2.1.5) into (2.1.1a), (2.1.1b) and (2.1.1c) we get the following nonlinear coupled ODEs

$$\left(\frac{\rho\mu}{\rho_0\mu_0} f''\right)' - Mf' - \beta (f')^2 + ff'' = 0, \tag{2.1.6a}$$

$$\left(\frac{\rho k}{\rho_0 k_0}\theta'\right)' + \frac{C_p}{C_{p0}} Pr_0 (\theta' f - \frac{2n}{1+m}\theta f') = 0, \tag{2.1.6b}$$

where Pr_0, β, M shows Prandtl number at temperature T_0, velocity ratio parameter and magnetic parameter respectively. These parameters are defined as
$Pr_0 = \frac{\mu_0 C_{p0}}{k_0}$, $\beta = \frac{2m}{1+m}$, M=$\frac{2\beta_0^2 \sigma}{\rho a(1+m)x^{m-1}}$.
After transformation the boundary conditions (2.1.2) take the form

$$\begin{aligned} f(0) = 0, \quad f'(0) = 1, \quad \theta(0) = 1, \\ f' \to 0, \quad \theta \to 0 \quad as \quad \eta \to \infty \end{aligned} \tag{2.1.7}$$

where f' denotes dimensionless velocity and θ denotes dimensionless temperature. The skin friction coeffcient C_f and local Nusselt number Nu_x are defined as follows Mustafa [20]:

$$C_f = \frac{\tau_w}{\rho U_w^2}, \quad Nu_x = \frac{x q_w}{T_w - T_0}, \tag{2.1.8}$$

where τ_w is the shear stress and q_w regarded as the heat flux, and are defined as :

$$\tau_w = \mu_w x^{\frac{3m-1}{2}} \sqrt{\frac{(1+m)a^3}{2\nu_0}} f''(0), \qquad q_w = \mu_w C_p \Delta T Pr_w^{-1} \sqrt{\frac{a(1+m)}{2\nu_0}} [-\theta'(0)], \tag{2.1.9}$$

using equation (2.1.8) and (2.1.9) we get

$$C_f Re^{1/2} = \sqrt{\frac{1+m}{2}} f''(0), \qquad Nu_x Re^{-1/2} = k_w \sqrt{\frac{1+m}{2}} [-\theta'(0)], \tag{2.1.10}$$

where Re denotes the local Reynolds number.

It should be noted that all the fluid properties considered here are constant execpt the viscosity which is temperature dependent. Following cases are discussed here as mentioned in Andersson and Aarsaeth[7] .

2.2 Special Cases

Case A: Constant Fluid Properties

For this case we assume all the fluid properties as constant. The dimensionless variables η and stream function ψ take the following form:

$$\eta = \sqrt{\frac{a}{\nu_0}} y, \quad \psi = \rho_0 \sqrt{a\nu_0} x f(\eta). \tag{2.2.1}$$

Under above similarity variables, Eqs. (2.1.6a) and (2.1.6b) take the form:

$$f''' + ff'' - \beta f'^2 - Mf' = 0, \tag{2.2.2a}$$

$$\theta'' + Pr_0 (f\theta' - \frac{2n}{1+m} f'\theta) = 0, \tag{2.2.2b}$$

the boundary conditions given in Eq. (2.1.7) remains the same.

Case B: Variable Viscosity (Inverse Relation with Temperature)

For this case, we assume only viscosity as a variable that depends linearly on temperature while treating the remaining fluid properties constant which is already explored in Andersson and Aarseth [7], Bachok et al [9], Elbashbeshy and Bazid

[18].

For this case the momentum boundary layer Eq. (2.1.6a) becomes

$$(f''\frac{\mu}{\mu_0})' + ff'' - \beta f'^2 - Mf' = 0. \tag{2.2.3}$$

The inverse linear relation between viscosity and temperature is proposed by Lai and Kulachi [8], Pop et al [12] and Ling and Dybbs [19]. The following is the relation

$$\mu = \frac{\mu_0}{1 - \frac{T-T_0}{\theta_{ref}(T_w - T_0)}} = \frac{\mu_0}{1 - \frac{\theta(\eta)}{\theta_{ref}}}, \tag{2.2.4}$$

By inserting Eq. (2.2.4) into Eq. (2.2.3), the resultant equation takes the following form

$$f''' + \frac{\theta'}{\theta_{ref} - \theta} f'' + (\frac{\theta_{ref} - \theta}{\theta_{ref}})(ff'' - Mf' - \beta f'^2) = 0. \tag{2.2.5}$$

Case C: Variable Viscosity (Exponential Relation with Temperature)

Similar to Case B, viscosity is again taken as variable and its exponential relation with temperature takes the following form White [36]:

$$\ln(\frac{\mu}{\mu_{ref}}) = -2.10 - 4.45\frac{T_{ref}}{T} + 6.55(\frac{T_{ref}}{T})^2. \tag{2.2.6}$$

Substituting the above formula Eq. (2.2.6) in Eq. (2.2.3) we get the following equation:

$$f''' = -f''\theta'\Delta T(4.45\frac{T_{ref}}{T^2} - 13.1\frac{T_{ref}^2}{T^3}) + \frac{\mu_0}{\mu}(\beta f'^2 - ff'' + Mf'). \tag{2.2.7}$$

2.3 Numerical Procedure

Here, we solved the nonlinear ordinary differential equations (ODEs) numerically for each Cases A, B and C with the boundary conditions in Eq. (2.1.7). For this

purpose we use shooting technique. The basic aim behind the shooting technique is to transform the BVP (boundary value problem) into an IVP (initial value problem). A fifth order Runge-Kutta method and root finding algorithm Newton-Raphson method are used to obtain solution of the transformed problem. We verify the results obtained from shooting technique with *bvp4c* [24] which is a built-in solver in MATLAB. Let us define the variables

$$y_1 = f \tag{2.3.1a}$$

$$y_2 = f' \tag{2.3.1b}$$

$$y_3 = f'' \tag{2.3.1c}$$

$$y_4 = \theta \tag{2.3.1d}$$

$$y_5 = \theta' \tag{2.3.1e}$$

(a) Case A: The system of first order momentum and energy equations for this case becomes

$$y_1' = y_2, \quad y_2' = y_3$$

$$y_3' = f''' = -y_1 y_3 + \beta y_2^2 + M y_2 \tag{2.3.2}$$

$$y_4' = y_5$$

$$y_5' = \theta'' = Pr_0 \left(\frac{2n}{m+1} y_2 y_4 - y_1 y_5 \right). \tag{2.3.3}$$

(b) Case B: For this case the y_3' takes the form,

$$y_3' = \frac{y_3 y_5}{0.25 + y_4} + \frac{0.25 + y_4}{0.25} (\beta y_2^2 + M y_2 - y_1 y_3), \tag{2.3.4}$$

(c) Case C: For this case the y_3' takes the form ,

$$y_3' = -y_3 y_5 \Delta T (4.45 \frac{T_{ref}}{T^2} - 13.1 \frac{T_{ref}^2}{T_3}) + \frac{\mu_0}{\mu} (\beta y_2^2 - y_1 y_3 + M y_2), \tag{2.3.5}$$

$$\frac{\mu}{\mu_0} = \frac{\mu_{ref}}{\mu_0} exp(-2.10 - 4.45(\frac{T_{ref}}{T}) + 6.65(\frac{T_{ref}}{T})^2). \tag{2.3.6}$$

We use these values in our calculations i.e. $\mu_{ref} = 0.001792kg/ms$, $\mu_0 = 0.001520kg/ms$, $T_{ref} = 273K$ and $T_0 = 278K$. The energy equations for Cases B and C unaltered as Eq. (2.3.3).

2.4 Results and Discussion

Numerical results for profiles of velocity and temperature are discussed in this part. Results are displayed in tabular and graphical form. Numerical solutions for skin friction $-f''(0)$ and temperature gradient $-\theta'(0)$ for different physical parameters are presented in different tables. From Tables 2.1, 2.4 and 2.5 one can observe that skin friction enhances whereas there is reduction in wall temperature as we raise magnetic parameter. The effect of Prandtl number and temperature index parameter is to enhance wall temperature while skin friction changes slightly. Wall temperature reduces while skin friction enhances with increase in stretching parameter. In Table 2.2 and 2.3, Nusselt number is calculated and compared with previously obtained results by Mustafa [20] and Ali [23]. The effects of Prandtl number are shown in Table 2.6. The skin friction coefficient increases for Case B while it changes slightly for both Case A and C but wall temperature enhances for all cases.

Table 2.1 – Values of $-f''(0)$ and $-\theta'(0)$ for different parameters (Case A).

					bvp4c		shooting method	
Pr	M	β	m	n	$-f''(0)$	$-\theta'(0)$	$-f''(0)$	$-\theta'(0)$
0.7	0.5	1	1	1	1.2247449	0.73595707	1.2247449	0.73683412
1	-	-	-	-	1.2247449	0.94089967	1.2247449	0.94099339
3	-	-	-	-	1.2247449	1.8655031	1.2247449	1.865517
7	-	-	-	-	1.2247449	3.0156599	1.2247449	3.0156921
10	-	-	-	-	1.2247449	3.6645662	1.2247449	3.6646523
0.7	0.1	-	-	-	1.0488089	0.78093708	1.0488089	0.78096049
-	0.2	-	-	-	1.0954451	0.76886566	1.0954451	0.76886391
-	0.3	-	-	-	1.1401754	0.75737841	1.1401754	0.75737874
-	0.4	-	-	-	1.183216	0.74642739	1.183216	0.7464299
10	0.5	0	0	-	0.9294730	4.8059057	0.92947343	4.8060571
-	-	1	1	-	1.2247449	3.6645669	1.2247449	3.6646523
-	-	1.33	2	-	1.3090637	3.2282285	1.3090635	3.2282143
-	-	1.6	4	-	1.3745053	2.8494207	1.3745033	2.8493841
-	-	1.75	7	-	1.4096676	2.6226409	1.4096386	2.6223442
1	0.1	1	1	0	1.0488089	0.57191381	1.0488089	0.5719128
-	-	-	-	1	1.0488089	0.98710811	1.0488089	0.98710798
-	-	-	-	2	1.0488089	1.3196014	1.0488089	1.319591

Table 2.2 – Comparison of ${C_f}{Re_x}^{1/2}$ and ${Re_x}^{-1/2}Nu_x$ for Pr=1 and M=0.

m	Mustafa[20]		Present results	
	$Re_x^{1/2}\,C_f$	$Re_x^{-1/2}\,Nu_x$	$Re_x^{1/2}\,C_f$	$Re_x^{-1/2}\,Nu_x$
0	-0.44375	0.44375	-0.443749	0.443749
1	-1.00000	1.00000	-1.00000	1.00000
2	-1.34845	1.34845	-1.34727	1.34866

Table 2.3 – Comparison of $Re_x^{-1/2} Nu_x$ when n=0, m=0, M=0 but for different values of Prandtl number.

Pr	Jacobi[21] (1993)	Tsou et al [22] (1969)	Ali[23] (1975)	Present results
0.7	0.3492	0.3492	0.3476	0.3492
1	0.4438	0.44378	0.4416	0.4437
10	1.6790	1.6804	1.6713	1.6803

Table 2.4 – Results for wall skin friction $-f''(0)$ and wall temperature gradient $-\theta'(0)$ with various values of M (Case B).

					bvp4c		shooting method	
M	Pr	β	n	m	$-f''(0)$	$-\theta'(0)$	$-f''(0)$	$-\theta'(0)$
0.1	1	1	1	1	2.4530235	0.72122229	2.4530188	0.72122789
0.2	-	-	-	-	2.5560358	0.69757654	2.5560372	0.69761235
0.3	-	-	-	-	2.6543977	0.67648866	2.6545432	0.67718638
0.4	-	-	-	-	2.7488177	0.6574893	2.7492952	0.65959234
0.5	-	-	-	-	2.8397797	0.63998507	2.8406015	0.64360739

Table 2.5 – Results for wall skin friction $-f''(0)$ and wall temperature gradient $-\theta'(0)$ with various values of M and Prandtl number Pr (Case C).

					bvp4c		shooting method	
Pr	M	β	m	n	$-f''(0)$	$-\theta'(0)$	$-f''(0)$	$-\theta'(0)$
0.7	0.5	1	1	1	2.7086855	0.48648367	2.71058	0.493869
1	-	-	-	-	2.7457538	0.66567042	2.74649	0.668392
3	-	-	-	-	2.9504369	1.5479812	2.95042	1.54797
7	-	-	-	-	3.2162104	2.6638754	3.21623	2.66385
10	-	-	-	-	3.3541575	3.294594	3.35427	3.29451
0.7	0	-	-	-	2.2358724	0.57909873	2.23586	0.579088
-	0.2	-	-	-	2.4376711	0.53485144	2.43782	0.535475
-	0.4	-	-	-	2.6217411	0.500965	2.62341	0.507445
-	0.5	-	-	-	2.7086796	0.48648475	2.71058	0.493869
-	1	-	-	-	3.1053418	0.42979585	3.1211	0.490544

Table 2.6 – Results for wall skin friction $-f''(0)$ and wall temperature gradient $-\theta'(0)$ with different values of Pr for n=1 and M=0.1 (Cases A, B and C).

			bvp4c		shooting method	
Cases	M	Pr	$-f''(0)$	$-\theta'(0)$	$-f''(0)$	$-\theta'(0)$
	0.1	0.7				
CaseA			1.0488089	0.78093708	1.0488089	0.78093637
CaseB			2.4220867	0.53201823	2.4220857	0.532034
CaseC			2.3394334	0.55518512	2.33943	0..555191
	0.1	1				
CaseA			1.0488089	0.98710811	1.0488089	0.98710798
CaseB			2.4530225	0.72122065	2.4530162	0.72121671
CaseC			2.3782471	0.7485637	2.37824	0.748559
	0.1	10				
CaseA			1.0488088	3.7084043	1.0488088	3.7085551
CaseB			2.9649588	3.3619367	2.9649931	3.3619032
CaseC			2.9378748	3.3920765	2.93794	3.39204

The effect of viscosity for all the three cases have been studied. Temperature of ambient fluid is $T_0 = 278K$ while temperature of surface is taken as $T_w = 358K$. In Figs 2.1 and 2.2, profiles for velocity and temperature are presented for all Cases A, B and C. In comparison with Case A and C velocity profile for Case B have been reduced adjacent to moving surface as shown in Fig 2.1. The viscosity of fluid adjacent to the surface reduces because of heat transfer. Comparing with the Case B temperature profile for both Cases A and C decreases close to moving surface as shown in Fig 2.2. Impact of magnetic parameter M on profiles of temperature and velocity have been shown in Figs (2.3-2.8). Temperature profile increases as we increase M and there is decreasing effect on momentum boundary layer for all three Cases A, B and C.

From Figs (2.9-2.14), the influence of β (stretching parameter) on velocity profile have been depicted. It can be seen that increment in β parameter causes momentum boundary layer to reduce, while there is an increment in thermal boundary layer for all cases. Physically, $\beta > 0$ shows that the surface is accelerating. The effect of temperature index parameter have been shown in Figs (2.15-2.20). For both Cases B and C, the momentum in the boundary layer becomes thicker while in Case A it has no effect. The thermal boundary layer shows a decreasing behaviour for all cases. Figs (2.21-2.26) shows the effect of Prandtl number on momentum and thermal boundary layer. For Case B and Case C, rise in Prandtl number causes increment in the momentum boundary layer whereas thermal boundary layer reduces for all cases by increasing Prandtl number but in Case A the velocity profile is not effected by Prandtl number because the momentum equation is decoupled from the energy equation due to which Prandtl number cannot influence velocity profile.

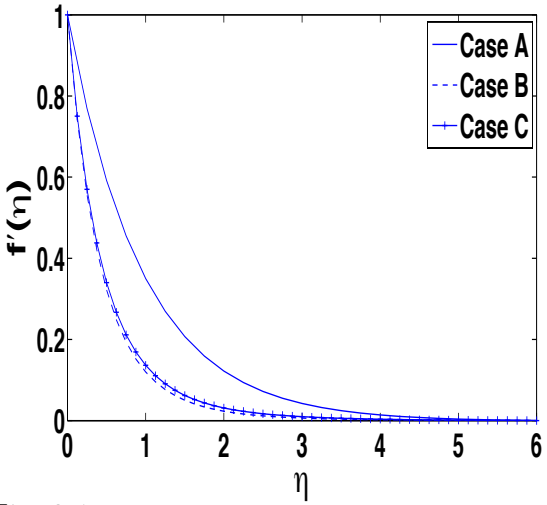

Fig. 2.1 – Variation in dimensionless velocity profiles $f'(\eta)$ for each Case.

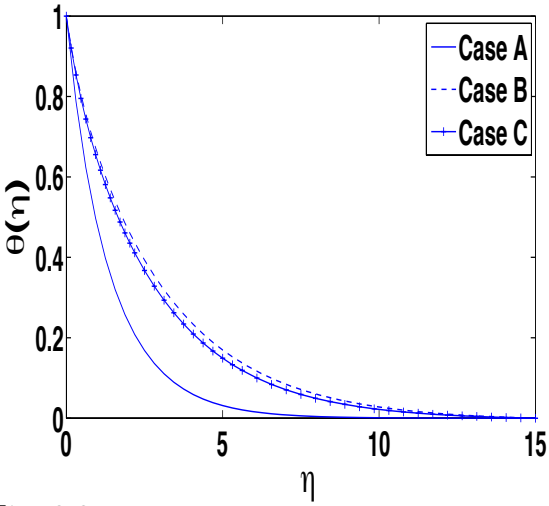

Fig. 2.2 – Variation in dimensionless temperature profiles $\theta(\eta)$ for each Case A, B and C with n=1 and M=0.1.

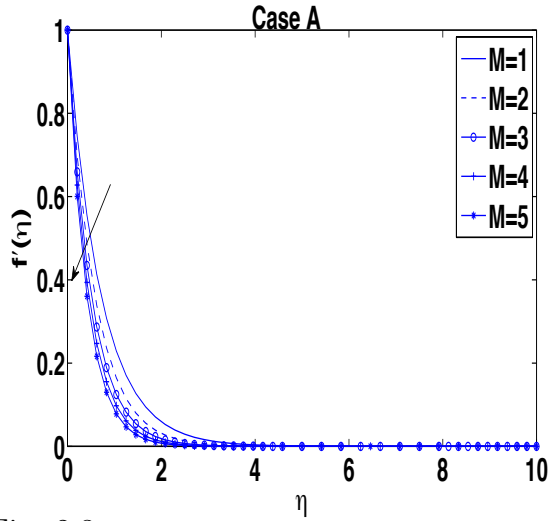

Fig. 2.3 – Variation in M and its impact on the dimensionless velocity profiles $f'(\eta)$ at $\beta = 1$, Pr=0.7 and n=1.

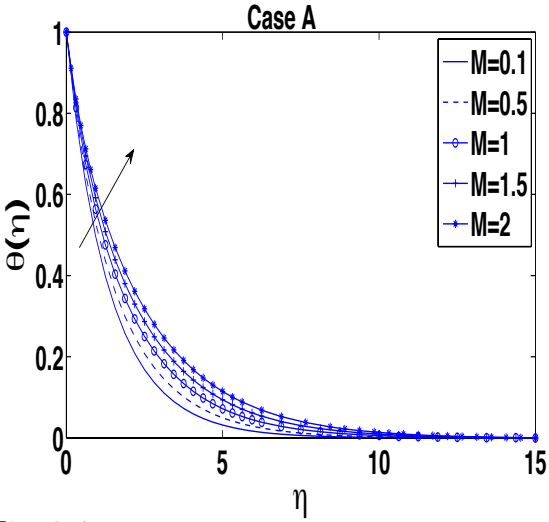

Fig. 2.4 – Variation in M and its impact on the dimensionless temperature profiles $\theta(\eta)$ at n=1, Pr=0.7 and $\beta = 1$.

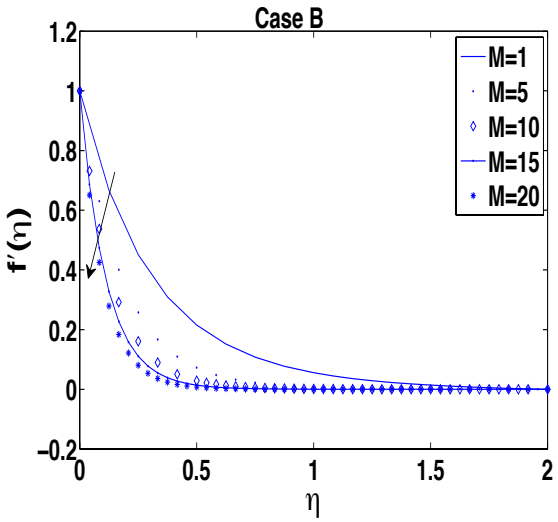

Fig. 2.5 – Variation in M and its impact on $f'(\eta)$ at n=1 and β=1.

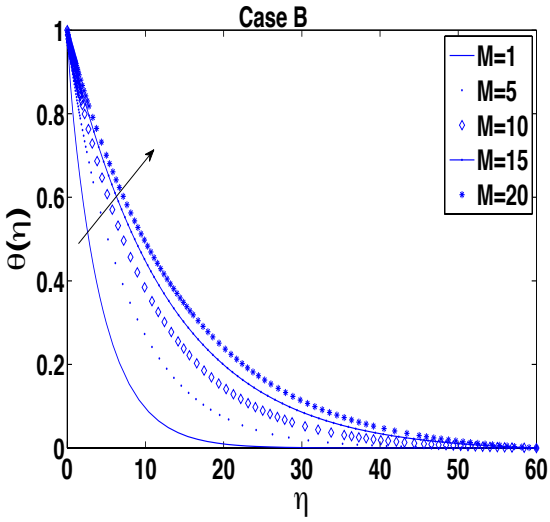

Fig. 2.6 – Variation in M and its impact on the dimensionless temperature profiles $\theta(\eta)$ at n=1 and β=1.

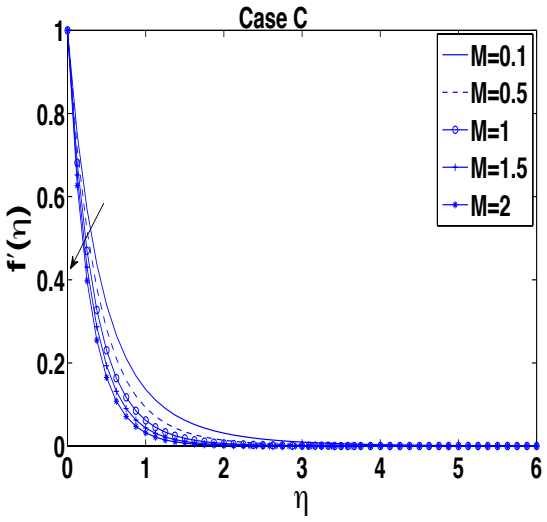

Fig. 2.7 – Variation in M and its impact on $f'(\eta)$ at n=1 and β=1.

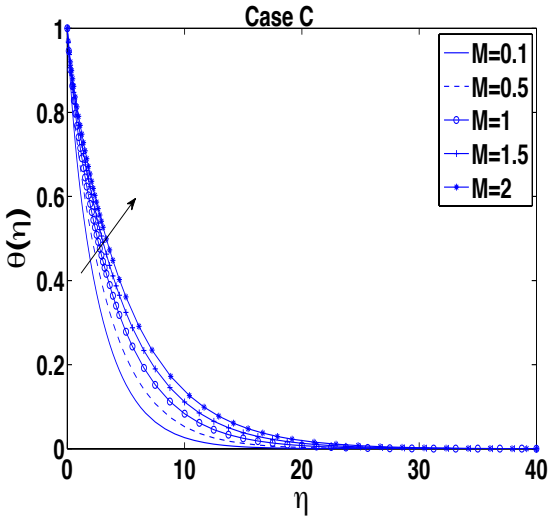

Fig. 2.8 – Variation in M and its impact on the dimensionless temperature profiles $\theta(\eta)$ at n=1 and β=1.

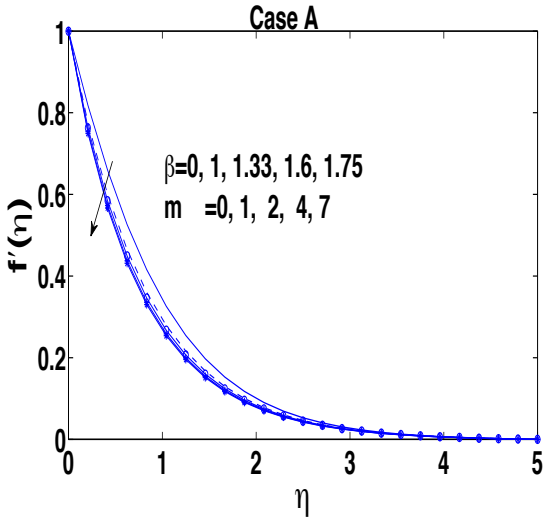

Fig. 2.9 – Variation of velocity profiles $f'(\eta)$ for different values of β at Pr=0.7.

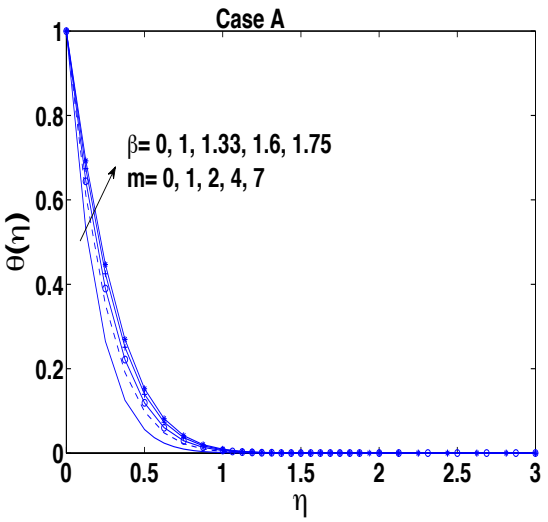

Fig. 2.10 – Variation of temperature profiles $\theta(\eta)$ for different values of β at Pr=0.7.

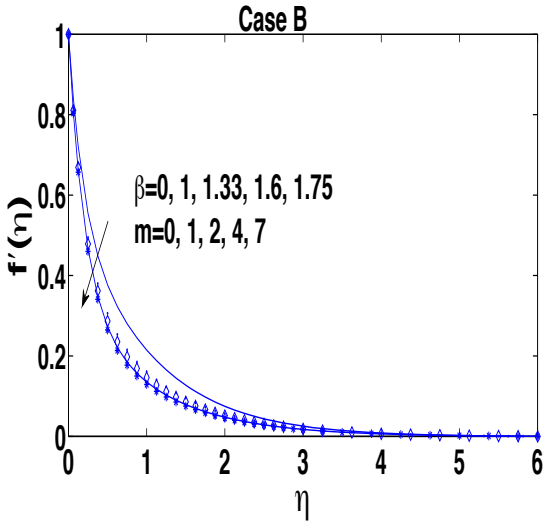

Fig. 2.11 – Variation of velocity profiles $f'(\eta)$ for different values of β at Pr=0.7.

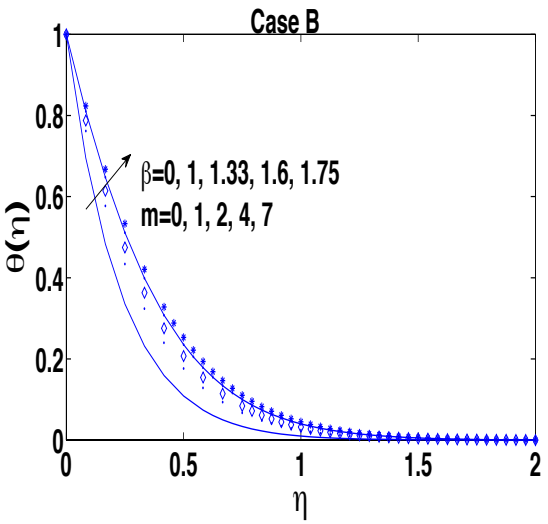

Fig. 2.12 – Variation of temperature profiles $\theta(\eta)$ for different values of β at Pr=0.7.

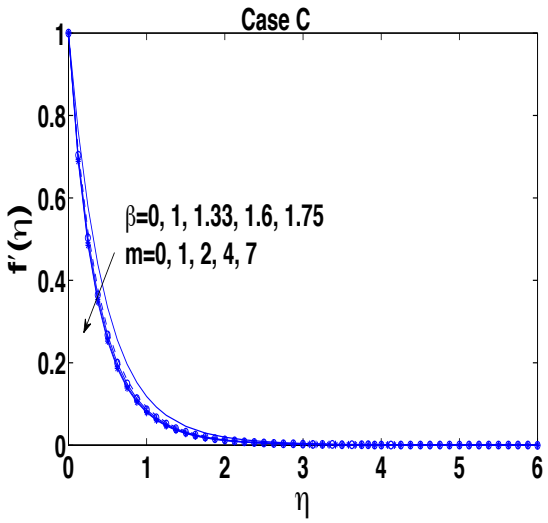

Fig. 2.13 – Variation of velocity profiles $f'(\eta)$ for different values of β at Pr=0.7.

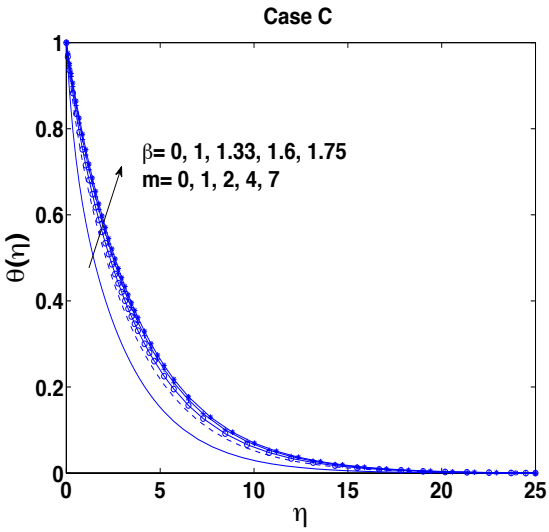

Fig. 2.14 – Variation of temperature profiles $\theta(\eta)$ for different values of β at Pr=0.7.

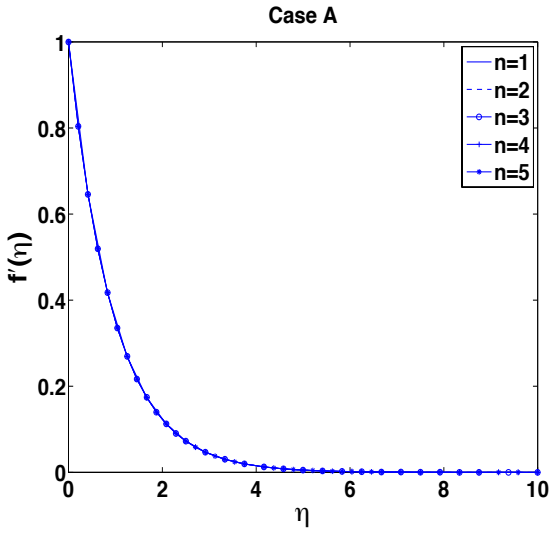

Fig. 2.15 – Variation in n and its impact on $f'(\eta)$ at m=1 and Pr=1.

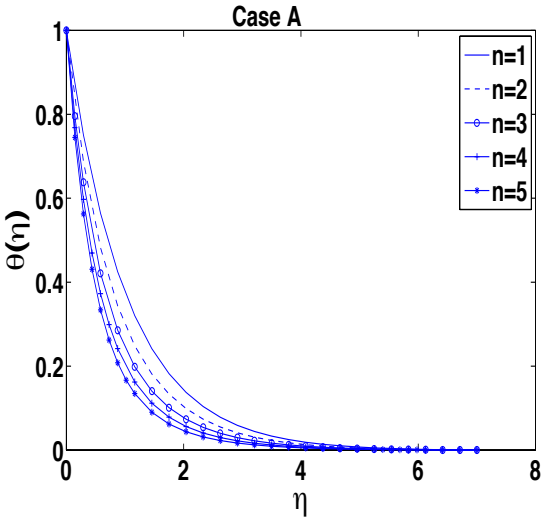

Fig. 2.16 – Variation in n and its impact on temperature curves at m=1 and Pr=1.

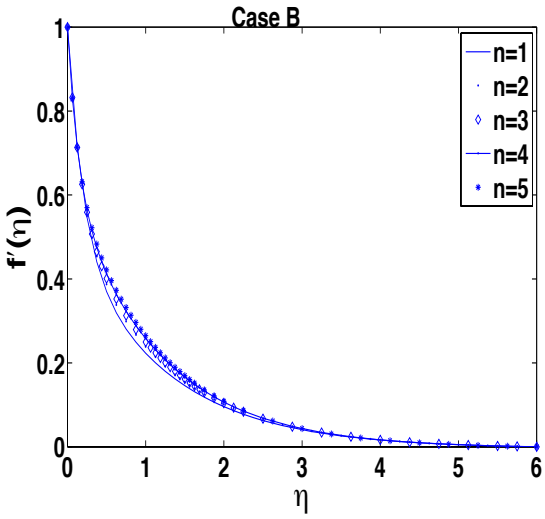

Fig. 2.17 – Variation in n and its impact on the dimensionless velocity profiles $f'(\eta)$ at m=1 and Pr=10.

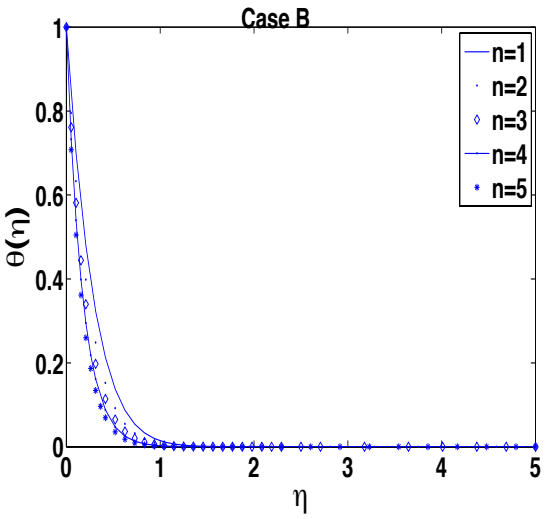

Fig. 2.18 – Variation in n and its impact on the dimensionless temperature profiles $\theta(\eta)$ at m=1 and Pr=10.

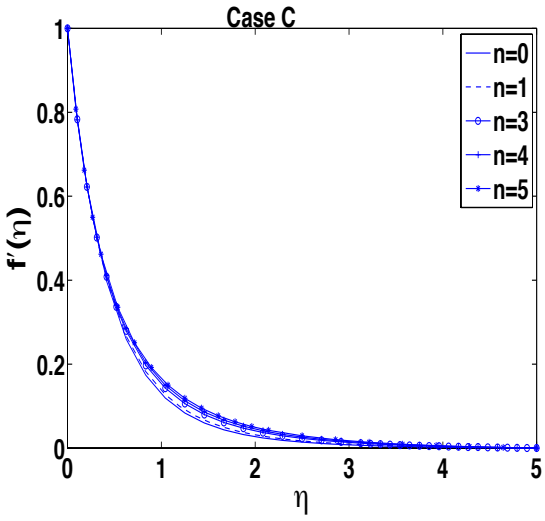

Fig. 2.19 – Variation in n and its impact on the dimensionless velocity profiles $f'(\eta)$ at m=1 and Pr=0.7.

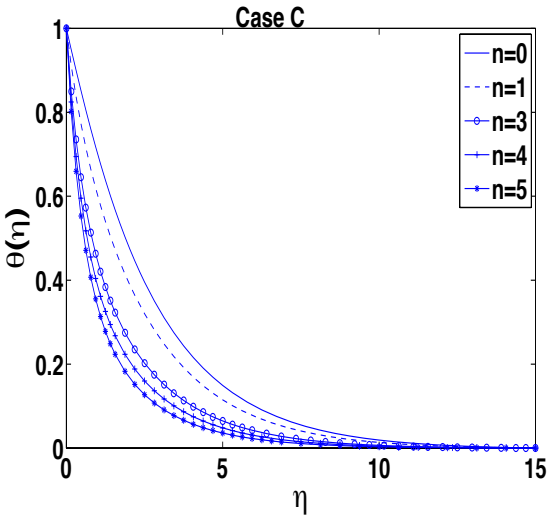

Fig. 2.20 – Variation in n and its impact on the dimensionless temperature profiles $\theta(\eta)$ at m=1 and Pr=0.7.

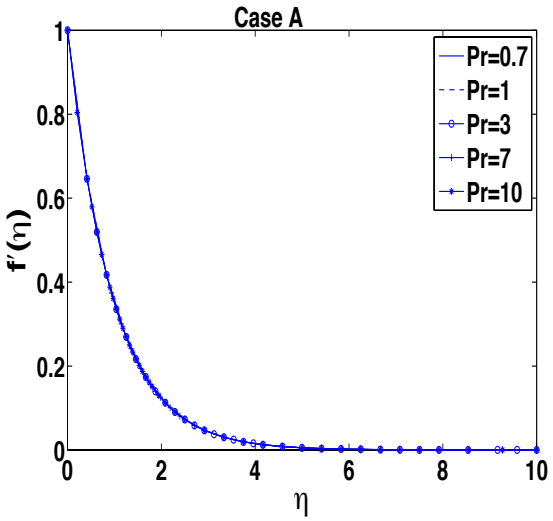

Fig. 2.21 – Variation of velocity profiles $f'(\eta)$ for different Pr_0 at M=0.1.

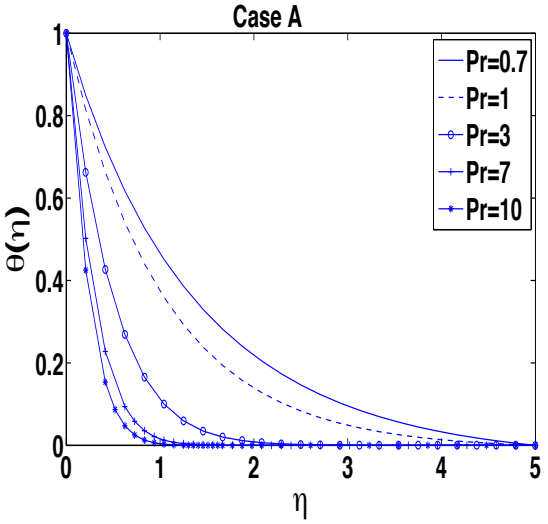

Fig. 2.22 – Variation of temperature profiles $\theta(\eta)$ for different Pr_0 at M=0.1.

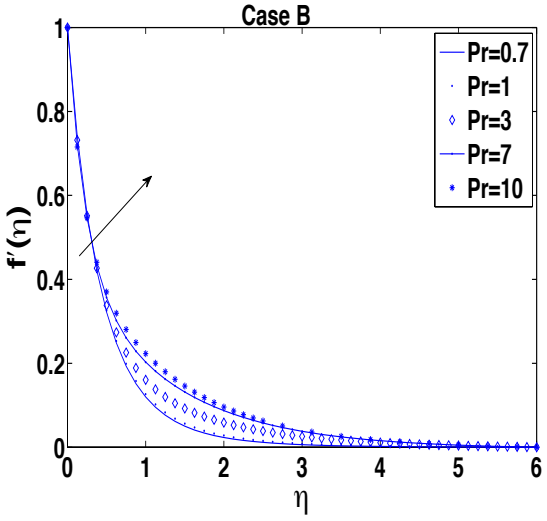

Fig. 2.23 – Variation in Pr and its impact on the dimensionless velocity profiles $f'(\eta)$ at M=0.1.

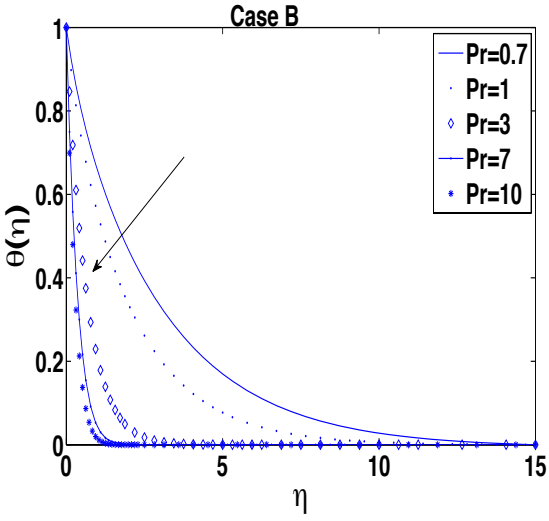

Fig. 2.24 – Variation in Pr and its impact on the dimensionless temperature profiles $\theta(\eta)$ at M=0.5.

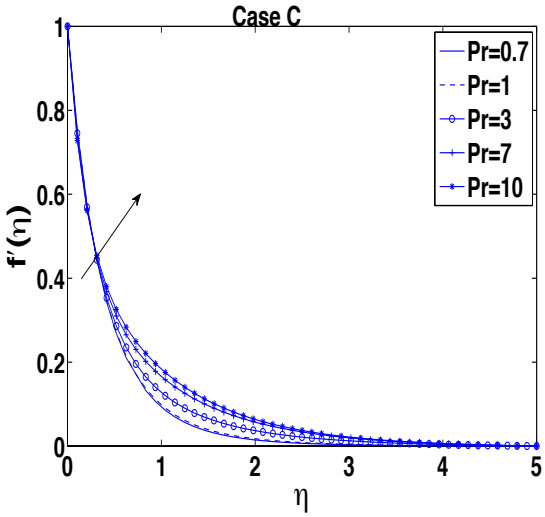

Fig. 2.25 – Variation in Pr and its impact on the dimensionless velocity profiles $f'(\eta)$ at M=0.5.

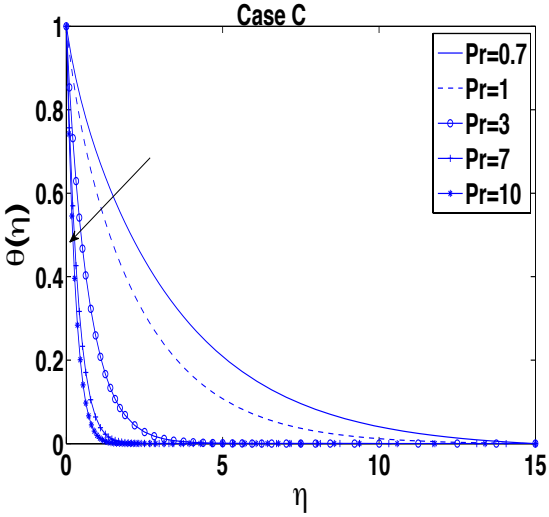

Fig. 2.26 – Variation in Pr and its impact on the dimensionless temperature profiles $\theta(\eta)$ at M=0.5.

2.5 Concluding Remarks

Skin friction coefficient and thermal boundary layer both increases with increment in magnetic parameter while velocity profile and wall temperature declines. Stretching parameter reduces momentum boundary layer for all cases whereas thermal boundary layer thickens. While results are opposite for skin friction and Nusselt number. Prandtl number causes thermal boundary layer to reduce whereas enhances momentum boundary layer. While it causes a slight change in skin friction and enhances wall temperature. The velocity profile increases in variable viscosity case but temperature profile decrease as we increase the temperature index parameter for all cases.

Chapter 3

Magnetohydrodynamics(MHD) Boundary Layer Flow and Heat Transfer Over an Exponentially Strecthing Surface with Variable Fluid Properties

In this chapter we explore the combined effects of variable viscosity and variable thermal conductivity on MHD flow of an incompressible viscous fluid. The present work is organized as follows. In Section 3.1 we present mathematical model for flow and heat transfer analysis. The special cases for the constant and variable viscosity and thermal conductivity have been discussed in Section 3.2. The computational procedure is given in Section 3.3. In Section 3.4 we present the graphs and tables and their discussion.

3.1 Problem Formulation

Here we consider a steady, laminar, two-dimensional, incompressible flow of an electrically conducting fluid. B_o is the strength of magnetic field which is applied normal to the sheet. Temperature of the sheet is T_w whereas the fluid is kept at temperature T_o. The flow-governing equations with these assumptions are given as Andersson and Aarsaeth [7]

$$\partial_x(\rho u) + \partial_y(\rho v) = 0, \tag{3.1.1a}$$

$$\rho(uu_x + vu_y) = \partial_y(\mu u_y) - \sigma B_0^2 u, \tag{3.1.1b}$$

$$\rho C_p(uT_x + vT_y) = \partial_y(kT_y), \tag{3.1.1c}$$

with boundary conditions

$$u(x,0) = U_w(x) = ae^{x/l}, \quad v(x,0) = 0, \quad T = T_w(x) = T_0 + ce^{bx/2l} \tag{3.1.2}$$
$$u \to 0, \quad T \to T_0, \quad as\ y \to \infty$$

here $[u, v]^T$ are the velocities along and normal to the surface. Fluid density is represented by ρ, B_0 shows applied magnetic field, μ is viscosity, specific heat is denoted by C_p, fluid's temperature is denoted by T and k represents thermal conductivity of the fluid. U_w represents the sheet's velocity, wall temperature is denoted by $T_w(x)$. Introducing the following similarity variables. Andersson and Aarsaeth [7]

$$\eta = \sqrt{\frac{a}{2\nu_0 L}} e^{x/2l} \int_0^y \frac{\rho}{\rho_0} dy, \qquad \psi = \rho_0 \sqrt{2a\nu_0 L} e^{x/2l} f(\eta), \qquad \theta(\eta) = \frac{T - T_0}{T_w - T_0} \tag{3.1.3}$$

stream function is denoted by ψ . Using Eq. (2.1.4) and (3.1.3) the x and y components of velocity can be written as

$$u = ae^{x/l} f'(\eta), \qquad v = -e^{x/2l} \sqrt{\frac{a\nu_0}{2l}} (\eta f' + f) \tag{3.1.4}$$

By using Eqs. (3.1.3) and (3.1.4) into (3.1.1a),(3.1.1b) and (3.1.1c) we get the following nonlinear (ODEs),

$$(\frac{\rho\mu}{\rho_0\mu_0}f'')' - 2Mf' - 2(f')^2 + ff'' = 0, \tag{3.1.5a}$$

$$(\frac{\rho k}{\rho_0 k_0}\theta')' + \frac{C_p}{C_{p0}}Pr_0(f\theta' - bf'\theta) = 0, \tag{3.1.5b}$$

where Pr, M shows Prandtl number and magnetic parameter respectively. These parameters are defined as: $\mathrm{Pr}_0=\frac{\mu_0 C_{p_0}}{k_0}$, $\mathrm{M}=\frac{\sigma B_0^2 l}{\rho_0 a e^{x/l}}$
After transformation the boundary conditions (3.1.2) taken the form :

$$\begin{aligned} f(0) = 0, \quad f'(0) = 1, \quad \theta(0) = 1, \\ f'(\eta) = 0, \quad \theta(\eta) = 0 \quad as \quad \eta \to \infty \end{aligned} \tag{3.1.6}$$

where f' denotes dimensionless velocity and θ denotes dimensionless temperature. It is important to note that all the fluid properties considered here are constant execpt the viscosity and thermal conductivity.

3.2 Special Cases

Case A: Constant Fluid Properties

For this case we assume all the fluid properties as constant. By using this assumption the momentum Eq. (3.1.5a) and energy Eq. (3.1.5b) becomes

$$f''' - 2f'^2 - 2Mf' + ff'' = 0, \tag{3.2.1}$$

$$\theta'' - Pr_0(bf'\theta - f\theta') = 0, \tag{3.2.2}$$

The conditions shown in Eq. (3.1.6) remain the same.

Case B: Variable Fluid Properties

For this case, we assume viscosity and thermal conductivity as variable that depend on temperature while keeping the remaining properties as constant. For this case the momentum boundary layer Eq. (3.1.5a) becomes

$$(f''\frac{\mu}{\mu_0})' + ff'' - 2f'^2 - 2Mf' = 0. \tag{3.2.3}$$

Energy equation (3.1.5b) becomes

$$(\frac{k}{k_0}\theta')' + Pr_0(f\theta' - bf'\theta) = 0. \tag{3.2.4}$$

Lai and Kulachi [8], Ling and Dybbs [19] and Pop et al [12] suggested the following relation between viscosity and temperature:

$$\mu(T) = \frac{\mu_{ref}}{[1 + \gamma(T - T_{ref})]},$$

If $T_{ref} \approx T_0$, the formula above becomes

$$\mu = \frac{\mu_0}{1 - \frac{T-T_0}{\theta_{ref}(T_w - T_0)}} = \frac{\mu_0}{1 - \frac{\theta(\eta)}{\theta_{ref}}}, \tag{3.2.5}$$

here $\theta_{ref} \equiv \frac{-1}{(T_w - T_0)\gamma}$ and $\Delta T = (T_w - T_0)$.
Using Eq. (3.2.5) in Eq. (3.2.3):

$$f''' - \left(\frac{\theta'}{\theta - \theta_{ref}}\right) f'' + \left(\frac{\theta_{ref} - \theta}{\theta_{ref}}\right((ff'' - 2f'^2 - 2Mf') = 0. \tag{3.2.6}$$

The thermal conductivity is defined as Subhas et. al [35]

$$k(T) = k_0(1 + \epsilon\theta),$$

$$\frac{k}{k_0} = 1 + \epsilon\theta, \tag{3.2.7}$$

using the above relation (3.2.7) in Eq. (3.2.4) we get the form.

$$(1 + \epsilon\theta)\theta'' + \epsilon\theta'^2 + Pr_0(f\theta' - bf'\theta) = 0. \tag{3.2.8}$$

Case C: Exponential Temperature Dependency

Like Case B, viscosity is again taken as variable. The relation of viscosity with temperature is taken from White [36] as explained in Chapter 2.
Substituting the Eq. (2.2.6) in Eq. (3.2.3) we get:

$$f''' = -f''\theta'\Delta T(4.45\frac{T_{ref}}{T^2} - 13.1\frac{T_{ref}^2}{T^3}) + \frac{\mu_0}{\mu}(2f'^2 - ff'' + 2Mf'). \tag{3.2.9}$$

while energy equation remains same as shown in Eq. (3.2.8).

3.3 Numerical Procedure

We apply shooting and bvp4c which has already been briefed in Chapter 1 and Chapter 2. The different cases takes the following form for imprementation purposes:
(a) Case A: Equations for momentum and energy becomes

$$y_3' = -y_1y_3 + 2y_2^2 + 2My_2, \tag{3.3.1}$$

$$y_5' = Pr_0(by_2y_4 - y_1y_5). \tag{3.3.2}$$

(b) Case B: For this case momentum equation becomes,

$$y_3' = \frac{y_3y_5}{0.25 + y_4} + \frac{0.25 + y_4}{0.25}(2y_2^2 + 2My_2 - y_1y_3). \tag{3.3.3}$$

Energy equation takes the form

$$y_5' = -\frac{1}{1 + \epsilon y_4}(\epsilon y_5^2 + Pr_0(y_1y_5 - by_2y_4)). \tag{3.3.4}$$

(c) Case C: Momentum equation becomes,

$$y_3' = -y_3y_5\Delta T(4.45\frac{T_{ref}}{T^2} - 13.1\frac{T_{ref}^2}{T_3}) + \frac{\mu_0}{\mu}(2y_2^2 - y_1y_3 + 2My_2). \tag{3.3.5}$$

here $\mu_{ref} = 0.001792kg/ms$, $\mu_0 = 0.001520kg/ms$, $T_{ref} = 273K$ and $T_0 = 278K$ while energy equation remains same as shown in Eq. (3.3.4).

3.4 Results and Discussions

In this part, results for velocity gradient and temperature gradient are discussed. Numerical solutions has been shown from Table 3.1 to 3.4. From Tables 3.1-3.3 one can observe that skin friction enhances whereas there is reduction in wall temperature as we raise magnetic parameter. Prandtl number enhance wall temperature for all the three cases while skin friction changes slightly. The parameter ϵ, reduces both the skin friction and wall temperature for both the Cases B and C. In Table 3.4 numerical results for $f'(0)$ and $\theta'(0)$ are computed for all cases by increasing the Prandtl number. Skin friction coefficient increases for Case B and C while for case A it shows decreasing behaviour. Wall temperature enhances for all the three cases. In Table 3.5 we compare our results with previous data.

Table 3.1 – $-f''(0)$ and $-\theta'(0)$ for different values of parameters for Case A.

		bvp4c		shooting method	
Pr	M	$f''(0)$	$\theta'(0)$	$f''(0)$	$\theta'(0)$
7	0	1.2818309	3.0131976	1.2818086	3.0132783
-	0.1	1.358984	2.29933966	1.3589569	2.993482
-	0.2	1.431606	2.9747289	1.4315737	2.2974817
-	0.3	1.5004709	2.9570449	1.5004643	2.9570699
-	0.4	1.5661991	2.9400727	1.5661916	2.9400974
3	0.1	1.3589814	1.8484702	1.3589571	1.8484698
5	-	1.3589801	2.4800045	1.3589569	2.480048
7	-	1.3589617	2.9934557	1.3589569	2.993482
10	-	1.3589615	3.6407616	1.3589569	3.6408323

Table 3.2 – $-f''(0)$ and $-\theta'(0)$ for different parameters for Case B.

			bvp4c		shooting method	
Pr	M	ϵ	$f''(0)$	$\theta'(0)$	$f''(0)$	$\theta'(0)$
7	0	0.1	3.3152541	2.4809717	3.3151441	2.4809382
-	0.1	-	3.4924239	2.4362617	3.492291	2.4362243
-	0.2	-	3.6546147	2.3955526	3.6544571	2.3955111
-	0.3	-	3.8056881	2.357806	3.8055048	2.3577602
-	0.4	-	3.9479607	2.3223623	3.9478457	2.322337
3	0.1	0.1	3.2777335	1.4022712	3.2776795	1.4022618
5	-	-	3.3945291	1.9723036	3.3944618	1.9722896
7	-	-	3.4923641	2.4362428	3.492291	2.4362243
10	-	-	3.6155618	3.0220062	3.6154815	3.0219747
7	0.1	0	3.5182186	2.6126496	3.5181387	2.6126254
-	-	0.1	3.4923641	2.4362428	3.492291	2.4362243
-	-	0.2	3.4690909	2.2865945	3.4690201	2.2865794

Table 3.3 – $-f''(0)$ and $-\theta'(0)$ for different values of parameters for Case C.

			bvp4c		shooting method	
Pr	M	ϵ	$f''(0)$	$\theta'(0)$	$f''(0)$	$\theta'(0)$
7	0	0.1	3.2681183	2.5090893	3.26809	2.50908
-	0.1	-	3.4411836	2.4668867	3.44115	2.46688
-	0.2	-	3.5993611	2.4282206	3.59932	2.42821
-	0.3	-	3.7462347	2.3922529	3.74619	2.39224
-	0.4	-	3.8841387	2.3584529	3.88408	2.35844
3	0.1	0.1	3.1992743	1.4325278	3.19924	1.43252
5	-	-	3.3332549	2.0025356	3.33321	2.00253
7	-	-	3.4411836	2.4668867	3.44115	2.46688
10	-	-	3.572496	3.053781	3.57247	3.05377
7	0.1	0	3.4698635	2.644825	3.46983	2.64481
-	-	0.1	3.4411836	2.4668867	3.44115	2.46688
-	-	0.2	3.4152734	2.3159895	3.41523	2.31598

Table 3.4 – Results of wall skin friction $-f''(0)$ and wall temperature gradient $-\theta'(0)$ for various Pr_0.

			bvp4c		shooting method	
Cases	M	Pr_0	$-f''(0)$	$-\theta'(0)$	$-f''(0)$	$-\theta'(0)$
	0.1	3				
CaseA			1.3589814	1.8484702	1.3589571	1.8484698
CaseB			3.2777335	1.4022712	3.2776795	1.4022618
CaseC			3.1992743	1.4325278	3.19924	1.43252
	0.1	5				
CaseA			1.3589801	2.4800045	1.3589569	2.480048
CaseB			3.3945291	1.9723036	3.3944618	1.9722896
CaseC			3.3332549	2.0025356	3.33321	2.00253
	0.1	7				
CaseA			1.3589617	2.9934557	1.3589569	2.993482
CaseB			3.4923641	2.4362428	3.492291	2.4362243
CaseC			3.4411836	2.4668867	3.44115	2.46688

Table 3.5 – Comparison of $\theta'(0)$ for M=0 and for various Prandtl numbers to previous data.

b	Pr	Magyari and Kellar [30]	Dulal Pal [37]	Present result
0.0	0.5	0.330493	0.33049	0.33049678
-	1	0.549643	0.54964	0.54965044
-	3	1.122188	1.12209	1.1220915
-	5	1.521243	1.52124	1.521232
1.0	0.5	0.594338	0.59434	0.59434314
-	1	0.954782	0.95478	0.95478975
-	3	1.869075	1.86907	1.8690695
-	5	2.500135	2.50013	2.5000639
3.0	0.5	1.008405	1.00841	1.0084165
-	1	1.560294	1.56030	1.5603051
-	3	2.938535	2.93854	2.9385528
-	5	3.886555	3.88656	3.8865662

The effect of viscosity and thermal conductivity for all the three cases have been studied. Temperature of ambient fluid is T_0= 278K while temperature of surface is taken as T_w= 358K. In Figs (3.1-3.2) velocity and temperature profiles are presented for all Cases A, B and C. In comparison with Case A and C velocity profile for Case B have been reduced adjacent to moving surface as shown in Fig 3.1 which shows same results for momentum boundary layer thickness. The viscosity of fluid adjacent to the surface reduces because of heat transfer. Comparing with the Case B temperature profile for both Cases A and C decreases close to moving surface as shown in Fig 3.2. Effect of M parameter(magnetic parameter), on temperature and velocity profile has been shown in Figs (3.3-3.8). Temperature profile increases as we increase M and there is decreasing effect on momentum boundary layer for all three Cases A, B and C. From Fig (3.9-3.12) the effect of Prandtl number has been shown. Wall temperature reduces for all the Cases A, B and C. While the velocity profile increases in Case B. In Fig (3.13-3.14) the effect of parameter ϵ on temperature profile has been shown. For both the Cases B and C there is an increment in temperature profile .

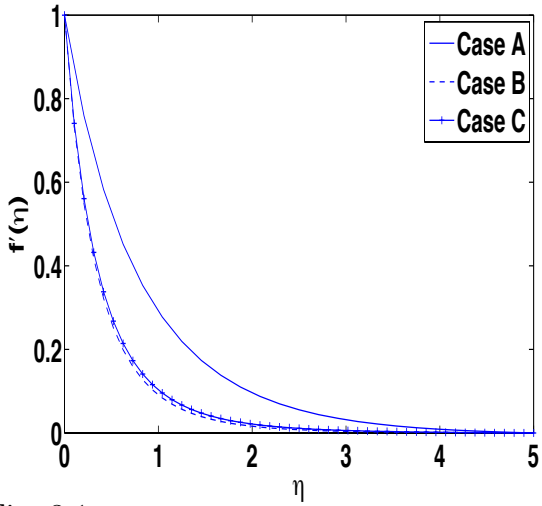

Fig. 3.1 – Velocity curves for each Case at Pr_0=0.7.

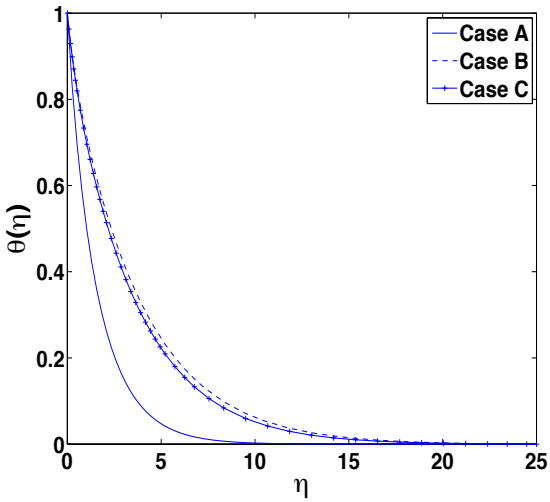

Fig. 3.2 – Dimensionless temperature profile for each Case at Pr_0=0.7.

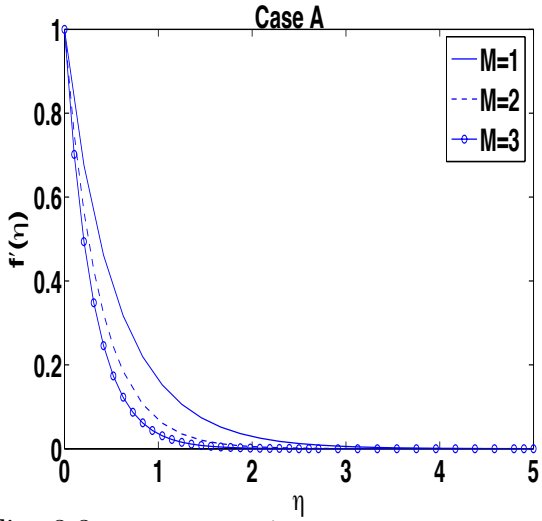

Fig. 3.3 – Values of $f'(\eta)$ for different M with Pr=3.

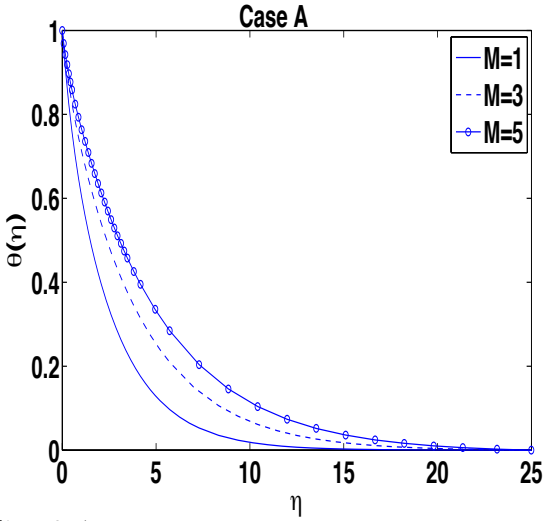

Fig. 3.4 – Values of $\theta'(\eta)$ for different M with Pr=3.

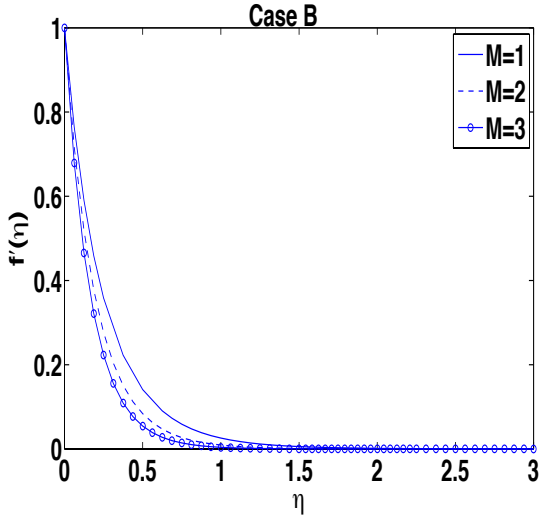

Fig. 3.5 – Values of $f'(\eta)$ for different M with ϵ=0.1 and Pr=3.

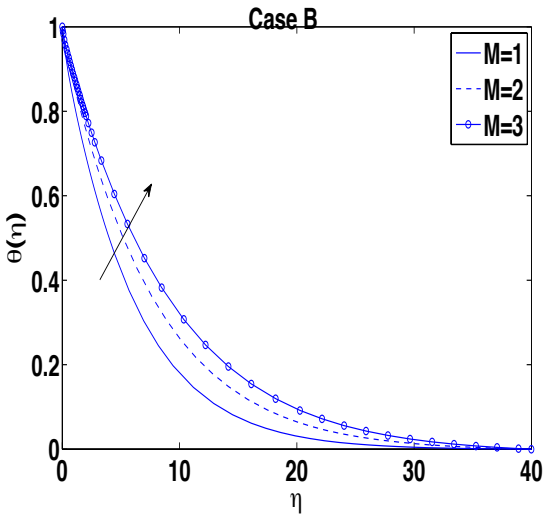

Fig. 3.6 – Values of $\theta'(\eta)$ for different M with ϵ=0.1 and Pr=3.

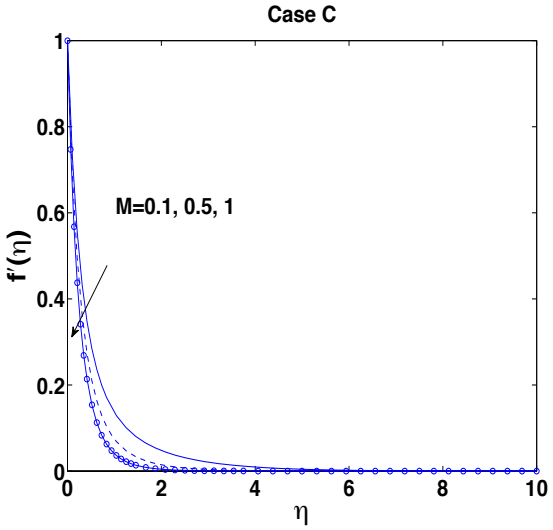

Fig. 3.7 – Velocity profiles for different values of M with ϵ=0.1 and Pr=3.

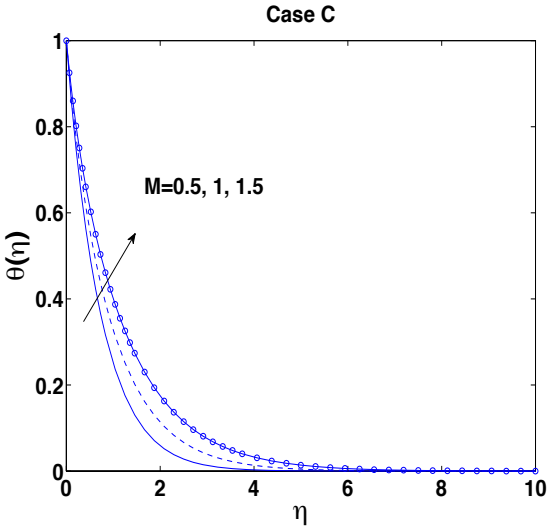

Fig. 3.8 – Temperature profiles for different values of M with ϵ=0.1 and Pr=3.

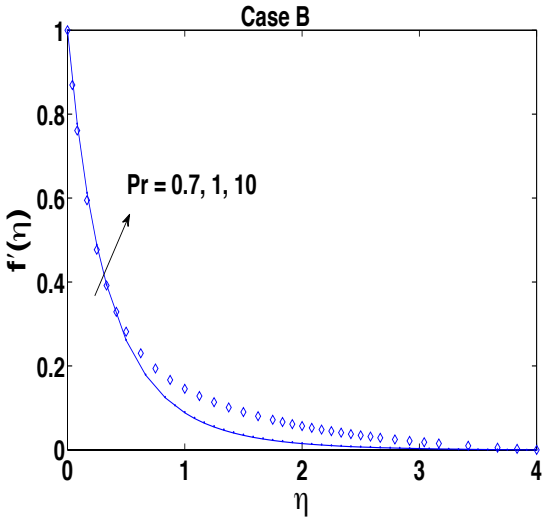

Fig. 3.9 – Dimensionless velocity profiles for different Pr_0.

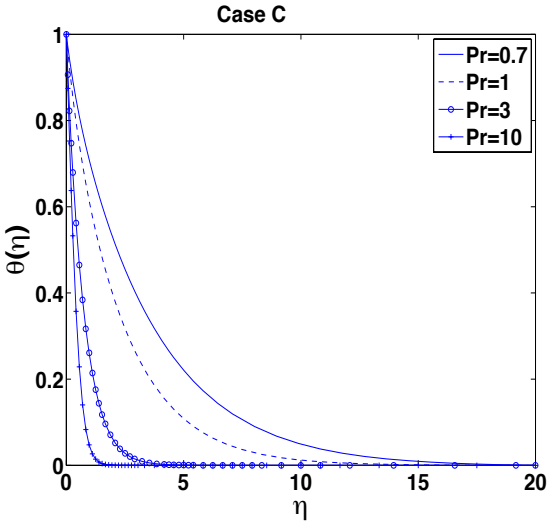

Fig. 3.10 – Dimensionless temperature profiles for different Pr_0.

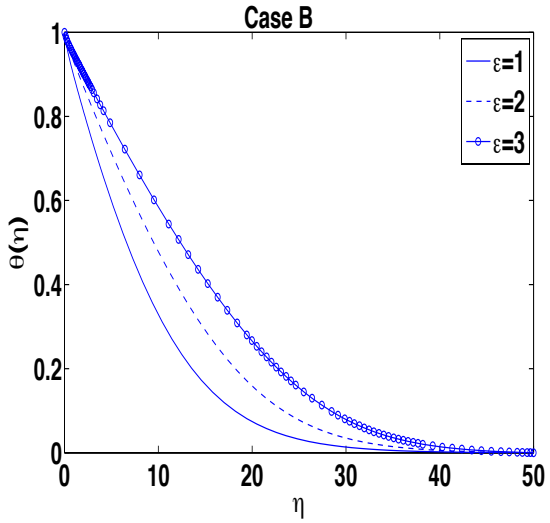

Fig. 3.11 – Temperature profiles for different values of parameter ϵ with Pr=0.7 and M=0.1.

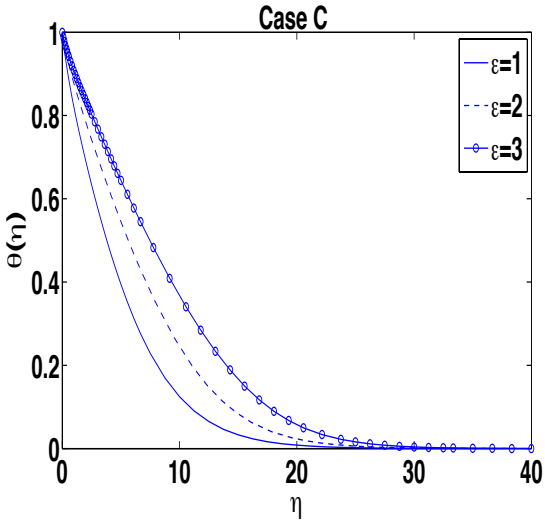

Fig. 3.12 – Temperature profiles for different values of parameter ϵ with Pr=0.7 and M=0.1.

3.5 Concluding Remarks

It is observed that skin friction and thermal boundary layer both increases with increment in magnetic parameter while velocity profile and wall temperature declines. Prandtl number causes a slight change in momentum boundary layer and skin friction whereas it enhances wall temperature and momentum boundary layer becomes thicker in case of variable viscosity. Thermal boundary layer reduces as Prandtl number rises. The parameter ϵ reduces both the skin friction and Nusselt number.

Chapter 4

Numerical Comparison of Constant and Variable Fluid Properties for MHD Flow of Nanofluid

4.1 Introduction

In this chapter we investigate the MHD flow of a nanofluid. Nanofluids have effective applications such as electronics, biomedical, transportation and much more. Nanofluid consist of ultra-fine particles (diameter less than 50 nm). Experimental results show that the thermal conductivity is appreciably improved by adding nanoparticles such as oxides, nitrides, carbides or nonmetals. The term nanofluid was proposed by Choi [38]. He showed that the thermal conductivity increases twice when nanoparticles are added to conventional base fluid.

We consider two case i.e. Constant (Case A) and Variable fluid properties (Case B). In Case B we assume viscosity and thermal conductivity as constant while keeping

remaining properties as constant. Different governing parameters and their impact on temperature, velocity and concentration profiles are discussed in detail.

4.2 Mathematical Formulation

Here we investigate a steady, 2-D and laminar MHD flow of an electrically conducting nanofluid over an exponentially stretching sheet. A magnetic field $B(x) = B_0 e^{x/2l}$ is applied normal to sheet. Using Buongiorno model, the governing equations take the following forms [41]:

$$\partial_x(\rho u) + \partial_y(\rho v) = 0, \tag{4.2.1}$$

$$\rho(uu_x + vu_y) = \partial_y(\mu u_y) - \sigma B^2 u, \tag{4.2.2}$$

$$(uT_x + vT_y) = \frac{1}{\rho C_p}\partial_y(kT_y) + \tau[D_B(C_y T_y) + \frac{D_T}{T_\infty}(T_y)^2], \tag{4.2.3}$$

$$uC_x + vC_y = D_B(C_{yy}) + \frac{D_T}{T_\infty}(T_{yy}), \tag{4.2.4}$$

here μ and ρ are coefficient of viscosity and mass density of the fluid respectively, σ is electrical conductivity, fluid's temperature is T, C denotes concentration, $\tau = (\rho C)_p/(\rho C)_f$ here $(\rho C)_p$, $(\rho C)_f$ are heat capacities of nanofluid and base fluid respectively, C_p is the specific heat at constant pressure, D_B is thermophoretic diffusion coefficient and D_T is Brownian coefficient. T_∞ denotes the temperature of ambient fluid and C_∞ is the concentration of ambient fluid.

4.3 Boundary Conditions

The appropriate BCs are as follows:

$$\begin{aligned} &u(x,0) = U_w, \quad v(x,0) = 0, \quad T(x,0) = T_w, \quad C(x,0) = C_w \\ &u \to 0, \quad T \to T_\infty, \quad C \to C_\infty \quad as\ y \to \infty. \end{aligned} \tag{4.3.1}$$

Here $U_w = U_0 e^{x/l}$ is the stretching velocity, U_0 is the reference velocity, $T_w = T_\infty + T_0 e^{x/(2l)}$ is the variable temperature at sheet with T_0 being a constant which measures the rate of temperature increase along the sheet and $C_w = C_\infty + C_0 e^{x/(2l)}$ is the variable concentration at the sheet with C_0 being a constant which measures the rate of concentration increase along the sheet.

4.4 Method of solution

The following similarity parameters are introduced to get nondimensionalized form of the momentum, energy and concentration equations as well as the boundary conditions.

$$\eta = \sqrt{\frac{U_0}{2\nu_0 L}} e^{x/2l} y, \quad \psi(\eta) = \sqrt{2U_0\nu_0 L} e^{x/(2l)} f(\eta) \tag{4.4.1}$$

$$\theta(\eta) = \frac{T - T_\infty}{T_0} e^{-x/(2l)}, \quad \phi(\eta) = \frac{C - C_\infty}{C_0} e^{-x/(2l)} \tag{4.4.2}$$

Where η is the similarity variable $\psi(\eta)$, $\theta(\eta)$ and $\phi(\eta)$ are dimensionless stream, temperature and concentration functions respectively. Stream function is defined as:

$$u = \frac{\partial \psi}{\partial y}, \qquad v = \frac{-\partial \psi}{\partial x} \tag{4.4.3}$$

Now we use Eqs. (4.4.1), (4.4.2) and (4.4.3) to find u and v.

$$u = U_0 e^{x/l} f'(\eta) \qquad v = -\sqrt{2U_0\nu_0 L} \frac{e^{x/2l}}{2L} (\eta f' + f) \tag{4.4.4}$$

We convert Eqs. (4.2.2), (4.2.3) and (4.2.4) into differential equations

$$\frac{\partial u}{\partial x} = U_0 \left(e^{x/l} f'' \sqrt{\frac{U_0}{2\nu_0 L}} \frac{e^{x/2l}}{2L} y + f' \frac{e^{x/l}}{L} \right)$$

$$\frac{\partial u}{\partial y} = U_0 e^{x/l} f'' \sqrt{\frac{U_0}{2\nu_0 L}} e^{x/2l}$$

$$\frac{\partial^2 u}{\partial^2 y} = U_0 e^{2x/l} \frac{U_0}{2\nu_0 L} f'''$$

$$u\frac{\partial u}{\partial x} = \left(U_0 e^{x/l} f'\right)\left(U_0 e^{x/l} f''\sqrt{\frac{U_0}{2\nu_0 L}}\frac{e^{x/2l}}{2L}y + \frac{U_0 f' e^{x/l}}{L}\right)$$

$$v\frac{\partial u}{\partial y} = \left(-\sqrt{2U_0\nu_0 L}\frac{e^{x/2l}}{2L}(\eta f' + f)\right)\left(U_0 e^{x/l} f''\sqrt{\frac{U_0}{2\nu_0 L}}e^{x/2l}\right)$$

$$\rho\left(u\frac{\partial u}{\partial x} + v\frac{\partial u}{\partial y}\right) = \rho\left(\frac{U_0^2}{L}e^{2x/l}f'^2 - \sqrt{2U_0\nu_0 L}\frac{e^{x/2l}}{2L}U_0 e^{x/l}\sqrt{\frac{U_0}{2\nu_0 L}}e^{x/2l}ff''\right) \quad (4.4.5)$$

$$\frac{\partial}{\partial y}\left(\mu\frac{\partial u}{\partial y}\right) = U_0 e^{2x/l}\frac{U_0}{2\nu_0 L}(\mu f'')'$$

$$\frac{\partial}{\partial y}\left(\mu\frac{\partial u}{\partial y}\right) - \sigma B^2 u = U_0 e^{2x/l}\frac{U_0}{2\nu_0 L}(\mu f'')' - \sigma B^2 u \quad (4.4.6)$$

By using Eq. (4.4.5) and (4.4.6) into Eq. (4.2.2) we get

$$\frac{\rho U_{0^2}}{L}(f')^2 - \rho\sqrt{2U_0\nu_0 L}\frac{e^{2x/l}}{2L}U_0\sqrt{\frac{U_0}{2\nu_0 L}}ff'' = U_0 e^{2x/l}\frac{U_0}{2\nu_0 L}(\mu f'')' - \sigma B^2 u$$

$$(\frac{\mu}{\mu_0}f'')' - Mf' - 2(f')^2 + ff'' = 0 \quad (4.4.7)$$

Here M is the magnetic parameter and its value is given by $M = \frac{2L\sigma B_0^2}{U_0\rho}$

Now by using Eq. (4.4.2) we find T and C.

$$T = \theta(\eta)T_0 e^{x/2l} + T_\infty$$

$$C = \phi(\eta)C_0 e^{x/2l} + C_\infty$$

$$\frac{\partial T}{\partial x} = T_0\left(\frac{\theta e^{x/2l}}{2L} + \theta'\sqrt{\frac{U_0}{2\nu_0 L}}\frac{e^{x/l}}{2L}y\right)$$

$$\frac{\partial T}{\partial y} = T_0 e^{x/l}\theta'\sqrt{\frac{U_0}{2\nu_0 L}}$$

$$\frac{\partial^2 T}{\partial y^2} = T_0 e^{3x/2l}\frac{U_0}{2\nu_0 L}\theta''$$

$$\frac{\partial C}{\partial y} = C_0 e^{x/l}\sqrt{\frac{U_0}{2\nu_0 L}}\phi'$$

$$u\frac{\partial T}{\partial x} = (U_0 f' e^{x/l})\left(\frac{T_0 e^{x/2l}\theta}{2L} + \frac{T_0 e^{x/l}}{2L}\sqrt{\frac{U_0}{2\nu_0 L}}\theta' y\right)$$

$$v\frac{\partial T}{\partial y} = \left(-\sqrt{\frac{U_0\nu_0}{2L}}e^{x/2L}(f'\eta + f)\right)\left(T_0 e^{x/l}\theta'\sqrt{\frac{U_0}{2\nu_0 L}}\right)$$

$$u\frac{\partial T}{\partial x}+v\frac{\partial T}{\partial y}=\frac{U_0T_0e^{3x/2l}}{2L}f'\theta-\frac{U_0T_0e^{3x/2l}}{2L}\theta' f \tag{4.4.8}$$

$$\frac{1}{\rho C_p}\frac{\partial}{\partial y}\left(k\frac{\partial T}{\partial y}\right)=\frac{1}{\rho C_p}\frac{\partial}{\partial y}\left(kT_0e^{x/l}\theta'\sqrt{\frac{U_0}{2\nu_0L}}\right) \tag{4.4.9}$$

$$=\frac{T_0e^{3x/2l}U_0}{2\rho C_p\nu_0L}\left(k\theta'\right)'$$

$$\tau\left(D_B\frac{\partial C}{\partial y}\frac{\partial T}{\partial y}+\frac{D_T}{T_\infty}\left(\frac{\partial T}{\partial y}\right)^2\right)=\tau\left(D_BC_0e^{2x/l}T_0\frac{U_0}{2\nu_0L}\phi'\theta'+\frac{D_T}{T_\infty}\left(T_0e^{x/l}\theta'\sqrt{\frac{U_0}{2\nu_0L}}\right)^2\right) \tag{4.4.10}$$

$$=\tau\left(\frac{D_BC_0T_0U_0}{2\nu_0L}e^{2x/l}\phi'\theta'+\frac{D_TT_0^2U_0}{2\nu_0LT_\infty}e^{2x/l}\theta'^2\right)$$

Adding Eqs. (4.4.9) and (4.4.10) we get

$$\frac{T_0e^{3x/2l}U_0}{2\rho C_p\nu_0L}\left(k\theta'\right)'+\tau\left(\frac{D_BC_0T_0U_0}{2\nu_0L}e^{2x/l}\phi'\theta'+\frac{D_TT_0^2U_0}{2\nu_0LT_\infty}e^{2x/l}\theta'^2\right) \tag{4.4.11}$$

By using Eq. (4.4.8) and (4.4.11) in Eq. (4.2.3) we get

$$\frac{U_0T_0}{2L}e^{3x/2l}\left(f'\theta-\theta' f\right)=\frac{U_0T_0}{2L\rho C_p\nu_0}e^{3x/2l}\left(k\theta'\right)'+\frac{U_0T_0C_0D_B}{2L\nu_0}e^{2x/l}\tau\phi'\theta'+\frac{U_0T_0^2D_T}{2L\nu_0T_\infty}e^{2x/l}\theta'^2$$

After solving above equation we get

$$\left(\frac{k}{k_0}\theta'\right)'+\frac{C_p}{C_{p_0}}Pr_0\left(Nb\phi'\theta'+Nt\theta'^2-f'\theta+\theta' f\right)=0 \tag{4.4.12}$$

Here Pr_0, Nt and Nb are Prandtl number, thermophoresis parameter and Brownian parameter respectively. These parameters are defined as

$$Pr_0=\frac{\mu_0C_{p0}}{k_0},\quad Nt=\frac{\tau D_T(T_w-T_\infty)}{T_\infty\nu_0},\quad Nb=\frac{\tau D_B(C_w-C_\infty)}{\nu_0}$$

Now consider

$$C=\phi(\eta)C_0e^{x/2l}+C_\infty \tag{4.4.13}$$

Differentiate (4.4.13) w.r.t 'x' and 'y'

$$\frac{\partial C}{\partial x} = C_0 \frac{e^{x/2l}}{2L}\phi + C_0 \frac{e^{x/l}}{2L}\sqrt{\frac{U_0}{2\nu_0 L}}y\phi'$$

$$\frac{\partial C}{\partial y} = C_0 e^{x/l}\sqrt{\frac{U_0}{2\nu_0 L}}\phi'$$

$$\frac{\partial^2 C}{\partial y^2} = C_0 \frac{U_0}{2\nu_0 L}e^{3x/2l}\phi''$$

$$u\frac{\partial C}{\partial x} + v\frac{\partial C}{\partial y} = \frac{U_0 C_0}{2L}e^{3x/2l}f'\phi - \frac{U_0 C_0}{2L}e^{3x/2l}f\phi' \tag{4.4.14}$$

$$D_B\left(\frac{\partial^2 C}{\partial y^2}\right) + \frac{D_T}{T_\infty}\left(\frac{\partial^2 T}{\partial y^2}\right) = D_B\left(\frac{C_0 U_0}{2\nu_0 L}e^{3x/2l}\phi''\right) + \frac{D_T}{T_\infty}\left(\frac{T_0 U_0}{2\nu_0 L}e^{3x/2l}\theta''\right) \tag{4.4.15}$$

By inserting Eq. (4.4.14) and (4.4.15) into Eq. (4.2.4) we get

$$\frac{U_0 C_0}{2L}e^{3x/2l}f'\phi - \frac{U_0 C_0}{2L}e^{3x/2l}f\phi' = \frac{U_0 C_0}{2\nu_0 L}D_B e^{3x/2l}\phi'' + \frac{T_0 U_0 D_T}{2\nu_0 L T_\infty}e^{3x/2l}\theta''$$

$$\phi'' + \frac{Nt}{Nb}\theta'' + Le\left(f\phi' - f'\phi\right) = 0 \tag{4.4.16}$$

After transformation the boundary conditions (4.3.1) takes the following form

$$f(\eta) = 0, \quad f'(\eta) = 1, \quad \theta(\eta) = 1, \quad \phi(\eta) = 1, \quad as \quad \eta \to 0 \tag{4.4.17}$$

$$f'(\eta) \to 0, \quad \theta(\eta) \to 0, \quad \phi(\eta) \to 0, \quad as \quad \eta \to \infty \tag{4.4.18}$$

The skin friction coeffcient C_f is given by [42]

$$C_f = \frac{\nu}{U_w^2}\left(\frac{\partial u}{\partial y}\right)_{y=0} \tag{4.4.19}$$

the local Nusselt number Nu_x is given by [42]

$$Nu_x = -\frac{x}{(T_w - T_\infty)}\left(\frac{\partial T}{\partial y}\right)_{y=0} \tag{4.4.20}$$

and the local Sherwood number Sh_x is given by [42]

$$Sh_x = -\frac{x}{(C_w - C_\infty)}\left(\frac{\partial C}{\partial y}\right)_{y=0} \tag{4.4.21}$$

After using the similarity transformations the equations (4.4.19), (4.4.20) and (4.4.21) becomes: [42]

$$C_f = \frac{1}{\sqrt{2Re_x}} f''(0)$$
$$Nu_x = -\sqrt{\frac{xRe_x}{2L}}\theta'(0)$$
$$Sh_x = -\sqrt{\frac{xRe_x}{2L}}\phi'(0)$$

Here $Re_x = Ux/\nu$ is a local Reynold number .

4.5 Special Cases

Case A: Constant Fluid Properties

For this case we assume all the fluid properties as constant. Under this assumption Eqs. (4.4.7), (4.4.12) and (4.4.16) take the form:

$$f''' - Mf' - 2f'^2 + ff'' = 0 \tag{4.5.1}$$

$$\theta'' + Pr_0(Nb\phi'\theta' + Nt\theta'^2 - f'\theta + \theta' f) = 0 \tag{4.5.2}$$

$$\phi'' + \frac{Nt}{Nb}\theta'' + Le(f\phi' - f'\phi) = 0 \tag{4.5.3}$$

the boundary conditions in Eq. (4.4.17) remains the same.

Case B: Variable Fluid Properties

For this case, we assume viscosity and thermal conductivity as variable while treating the remaining fluid properties constant. For this case the momentum Eq. (4.4.7) becomes:

$$(\frac{\mu}{\mu_0} f'')' - Mf' - 2(f')^2 + ff'' = 0, \tag{4.5.4}$$

The energy equation (4.4.12) becomes

$$(\frac{k}{k_0}\theta')' + Pr_0(Nb\phi'\theta' + Nt\theta'^2 - f'\theta + \theta' f) = 0, \tag{4.5.5}$$

The concentration equation (4.4.16) becomes

$$\phi'' + \frac{Nt}{Nb}\theta'' + Le(f\phi' - f'\phi) = 0, \tag{4.5.6}$$

Makinde et. al [39] suggested the following relation

$$\mu = \mu_0 e^{-\beta(T-T_\infty)}$$

$$\frac{\mu}{\mu_0} = e^{-\beta(T-T_\infty)} \tag{4.5.7}$$

By using Eq. (4.5.7) in Eq. (4.5.4) we get

$$\begin{aligned}
\left(e^{-\beta(T-T_\infty)} f''\right)' - Mf' - 2f'^2 + ff'' &= 0 \\
e^{-\beta(T-T_\infty)} f''' + f'' \frac{\partial}{\partial \eta}\left(e^{-\beta(T-T_\infty)}\right) - Mf' - 2f'^2 + ff'' &= 0 \\
e^{-\beta(T-T_\infty)} f''' - \beta T_0 e^{x/2l} f'' e^{-\beta(T-T_\infty)}\theta' + (-Mf' - 2f'^2 + ff'') &= 0
\end{aligned}$$

Divide by $e^{-\beta(T-T_\infty)}$ on both sides we get

$$\begin{aligned}
f''' - \beta(T-T_\infty)\frac{\theta'}{\theta} f'' + e^{\beta(T-T_\infty)}\left(-Mf' - 2f'^2 + ff''\right) &= 0 \\
f''' - \beta(T-T_\infty)\frac{T_w - T_\infty}{T_w - T_\infty}\frac{\theta'}{\theta} f'' + e^{\beta(T-T_\infty)\frac{T_w-T_\infty}{T_w-T_\infty}}\left(-Mf' - 2f'^2 + ff''\right) &= 0 \\
f''' - \beta(T_w - T_\infty)\theta\frac{\theta'}{\theta} f'' + e^{\beta(T_w-T_\infty)\theta}\left(-Mf' - 2f'^2 + ff''\right) &= 0 \\
f''' - \beta(T_w - T_\infty)\theta' f'' + e^{\beta(T_w-T_\infty)\theta}\left(-Mf' - 2f'^2 + ff''\right) &= 0 \\
f''' - \delta\theta' f'' + e^{\delta\theta}\left(-Mf' - 2f'^2 + ff''\right) &= 0
\end{aligned} \tag{4.5.8}$$

The thermal conductivity is defined as Hayat et. al [40]

$$k(T) = k_0(1 + \epsilon\theta)$$

$$\frac{k}{k_0} = (1 + \epsilon\theta) \tag{4.5.9}$$

By using the above relation (4.5.9) in Eq. (4.5.5) we get

$$\begin{aligned}((1+\epsilon\theta)\theta')' + \frac{C_p}{C_{p_0}} Pr_0 \left(N_b\phi'\theta' + N_t\theta'^2 - f'\theta + \theta' f\right) = 0 \\ (1+\epsilon\theta)\theta'' + \theta'(1+\epsilon\theta)' + Pr_0 \left(N_b\phi'\theta' + N_t\theta'^2 - f'\theta + \theta' f\right) = 0 \\ (1+\epsilon\theta)\theta'' + \epsilon(\theta')^2 + Pr_0 \left(N_b\phi'\theta' + N_t\theta'^2 - f'\theta + \theta' f\right) = 0 \end{aligned} \tag{4.5.10}$$

The concentration equation (4.5.6) remains the same.

4.6 Numerical Procedure

We apply shooting method and bvp4c for numerical solutions which are already explained in previous chapters. The different cases takes the following form:
(a) Case A: The system of first order momentum, energy and concentration equations for this case becomes

$$y_3' - My_2 - 2y_2^2 + y_1y_3 = 0 \tag{4.6.1}$$

$$y_5' + Pr_0(Nby_7y_5 + Nty_5^2 - y_2y_4 + y_5y_1) = 0 \tag{4.6.2}$$

$$y_7' + \frac{Nt}{Nb}y_5' + Le(y_1y_7 - y_2y_6) = 0 \tag{4.6.3}$$

(b) Case B: The system of first order momentum, and energy equations for this case becomes

$$y_3' - \delta y_5y_3 + e^{\delta\theta}(y_1y_3 - 2y_2^2 - My_2) = 0 \tag{4.6.4}$$

$$(1+\epsilon y_4)y_5' + \epsilon y_5^2 + Pr(Nby_7y_5 + Nty_5^2 - y_2y_4 + y_5y_1) = 0 \tag{4.6.5}$$

while the concentration equation remains the same.

4.7 Results and Discussion

Numerical results for profiles of velocity, temperature and concentration are discussed in this part. Results are displayed in tabular and graphical form. Numerical

solutions for skin friction $-f''(0)$ temperature gradient $-\theta'(0)$ and concentration gradient $-\phi'(0)$ for different physical parameters which includes Prandtl number Pr, Lewis number Le, magnetic parameter M, thermophoresis parameter Nt and viscosity variation parameter δ are presented in different Tables. From Tables 4.1-4.3, one can observe that skin friction enhances while there is reduction in both wall temperature gradient and concentration gradient as we raise magnetic parameter. Prandtl number causes slight change in skin friction while wall temperature enhances and concentartion gradient reduces. Thermophoresis parameter reduces both wall temperature and concentartion gradient for both Case A and Case B. There is no change in skin friction for Case A while for Case B it reduces as we raise Nt parameter. The Brownian motion parameter and Lewis number reduces wall temperature while the concentration gradient enhances for both Case A and B. The skin friction changes slightly for Case A while for Case B it reduces as Nb parameter increases. Lewis number causes reduction in skin friction for Case B while there is no change for Case A. Viscosity variation parameter causes increment in skin friction while both the wall temperature and concentration gradient reduces. The parameter ϵ reduces wall temperature and concentration gradient shows increment. It causes slight change in skin friction. In Table 4 results are compared with previoulsy published papers.

Table 4.1 – Results of $-f''(0)$, temperature gradient $-\theta'(0)$ and concentration gradient $-\phi'(0)$ for various parameters (Case A).

					bvp4c			shooting method		
M	Pr	Nt	Nb	Le	$-f''(0)$	$-\theta'(0)$	$-\phi'(0)$	$-f''(0)$	$-\theta'(0)$	$-\phi'(0)$
0	0.7	0.5	0.5	1	1.28183	0.60768	0.59384	1.28180	0.60768	0.59383
0.1	-	-	-	-	1.32104	0.60004	0.58055	1.32101	0.60004	0.58054
0.2	-	-	-	-	1.35895	0.59274	0.56809	1.35899	0.59275	0.56810
0.3	-	-	-	-	1.39581	0.58574	0.55638	1.39577	0.58574	0.55640
0.1	0.5	-	-	-	1.32104	0.49424	0.64988	1.32101	0.49424	0.64988
-	1	-	-	-	1.32104	0.72007	0.49942	1.32101	0.72007	0.49942
-	1.5	-	-	-	1.32104	0.86054	0.40161	1.32101	0.86053	0.40161
-	2	-	-	-	1.32104	0.95831	0.33212	1.32101	0.95830	0.33212
0.1	0.7	0.1	0.5	1	1.32104	0.63342	0.86658	1.32101	0.63342	0.86658
-	-	0.4	-	-	1..32104	0.60802	0.64888	1.32101	0.60801	0.64887
-	-	0.7	-	-	1.32104	0.58480	0.44957	1.32101	0.58480	0.44956
-	-	1	-	-	1.32104	0.56358	0.26581	1.32101	0.56358	0.26580
0.1	0.7	0.5	0.5	1	1.32104	0.60004	0.58055	1.32101	0.60004	0.58054
-	-	-	1	-	1.32104	0.52241	0.79208	1.32101	0.52241	0.79208
-	-	-	2	-	1.32104	0.39949	0.89077	1.32101	0.39949	0.89077
-	-	-	4	-	1.32102	0.24791	0.93021	1.32101	0.24791	0.93020
0.1	0.7	0.5	0.5	0.5	1.32104	0.63448	0.11977	1.32101	0.63448	0.119776
-	-	-	-	1	1.32104	0.60004	0.58055	1.32101	0.60004	0.58054
-	-	-	-	2	1.32104	0.56952	1.19407	1.32101	0.56952	1.19407
-	-	-	-	3	1.32104	0.55413	1.64332	1.32101	0.55413	1.64333

Table 4.2 – Results of $-f''(0)$, temperature gradient $-\theta'(0)$ and concentration gradient $-\phi'(0)$ for different parameters (Case B).

							bvp4c		
M	Pr	Nt	Nb	Le	δ	ϵ	$-f''(0)$	$-\theta'(0)$	$-\phi'(0)$
0	0.7	0.5	0.5	1	1	0.1	2.19690	0.47565	0.48136
0.1	-	-	-	-	-	-	2.26080	0.46328	0.46189
0.2	-	-	-	-	-	-	2.32242	0.45209	0.44513
0.3	-	-	-	-	-	-	2.38208	0.44182	0.43032
0.1	0.5	0.5	0.5	1	1	0.1	2.24253	0.36398	0.52636
-	1	-	-	-	-	-	2.28294	0.58220	0.38379
-	1.5	-	-	-	-	-	2.31056	0.72884	0.28538
-	2	-	-	-	-	-	2.33086	0.83606	0.21169
0.1	0.7	0.1	0.5	1	1	0.1	2.26530	0.48502	0.72148
-	-	0.4	-	-	-	-	2.26188	0.46847	0.52483
-	-	0.7	-	-	-	-	2.25873	0.45335	0.33953
-	-	1	-	-	-	-	2.25585	0.43954	0.16392
0.1	0.7	0.5	0.5	1	1	0.1	2.26080	0.46328	0.46189
-	-	-	1	-	-	-	2.25149	0.40889	0.64336
-	-	-	2	-	-	-	2.23640	0.32313	0.72670
-	-	-	4	-	-	-	2.21681	0.21667	0.75850
0.1	0.7	0.5	0.5	0.5	-	-	2.26472	0.48823	0.06519
-	-	-	-	1	-	-	2.26080	0.46328	0.46189
-	-	-	-	2	-	-	2.25802	0.44105	1.02863
-	-	-	-	3	-	-	2.25705	0.42992	1.45832
-	-	-	-	-	0	-	1.3210486	0.56410	0.60731
-	-	-	-	-	0.5	-	1.74097	0.51754	0.53831
-	-	-	-	-	1	-	2.26080	0.46328	0.46189
-	-	-	-	-	1.5	-	2.90518	0.40157	0.38119
-	-	-	-	-	-	0	2.26650	0.49704	0.43776
-	-	-	-	-	-	0.1	2.26080	0.46328	0.46189
-	-	-	-	-	-	0.2	2.25579	0.43418	0.48230

Table 4.3 – Results of $-f''(0)$, temperature gradient $-\theta'(0)$ and concentartion gradient $-\phi'(0)$ for different parameters (Case B).

								shooting method	
M	Pr	Nt	Nb	Le	δ	ϵ	$-f''(0)$	$-\theta'(0)$	$-\phi'(0)$
0	0.7	0.5	0.5	1	1	0.1	2.19684	0.47565	0.48135
0.1	-	-	-	-	-	-	2.26074	0.46327	0.46190
0.2	-	-	-	-	-	-	2.32236	0.45212	0.44553
0.3	-	-	-	-	-	-	2.38207	0.44198	0.43200
0.1	0.5	0.5	0.5	1	1	0.1	2.24248	0.36400	0.52642
-	1	-	-	-	-	-	2.28287	0.58219	0.38379
-	1.5	-	-	-	-	-	2.31047	0.72883	0.28537
-	2	-	-	-	-	-	2.33084	0.83606	0.21169
0.1	0.7	0.1	0.5	1	1	0.1	2.26524	0.48501	0.72147
-	-	0.4	-	-	-	-	2.26182	0.46846	0.52483
-	-	0.7	-	-	-	-	2.25868	0.45335	0.33955
-	-	1	-	-	-	-	2.25579	0.43954	0.16396
0.1	0.7	0.5	0.5	1	1	0.1	2.26074	0.46327	0.46189
-	-	-	1	-	-	-	2.25143	0.40889	0.64336
-	-	-	2	-	-	-	2.23635	0.32313	0.72670
-	-	-	4	-	-	-	2.21677	0.21667	0.75850
0.1	0.7	0.5	0.5	0.5	-	-	2.26464	0.48813	0.06586
-	-	-	-	1	-	-	2.26074	0.46327	0.46190
-	-	-	-	2	-	-	2.25797	0.44105	1.02862
-	-	-	-	3	-	-	2.25699	0.42991	1.45831
-	-	-	-	-	0	-	1.32101	0.56410	0.60730
-	-	-	-	-	0.5	-	1.74095	0.51754	0.53830
-	-	-	-	-	1	-	2.26074	0.46327	0.46190
-	-	-	-	-	1.5	-	2.90515	0.40158	0.38135
-	-	-	-	-	-	0	2.26643	0.49703	0.43775
-	-	-	-	-	-	0.1	2.26074	0.46327	0.46190
-	-	-	-	-	-	0.2	2.25574	0.43418	0.48231

Table 4.4 – The wall-temperature gradient for M=0 and for various Prandtl numbers to previous data.

a	Pr	Magyari and Kellar [13]	Dulal Pal [37]	Present result
1.0	0.5	0.594338	0.59434	0.59434314
-	1	0.954782	0.95478	0.95478975
-	3	1.869075	1.86907	1.8690695
-	5	2.500135	2.50013	2.5000639

In Fig 4.1 and 4.2 profiles for velocity and concentration are presented for both Case A and B. In comparison with Case A the velocity profile for Case B have been reduces while concentration profile have been increased. Impact of magnetic parameter M, on profiles of temperature, velocity and concentration has been shown in Figs (4.3-4.8). Temperature and concentration profiles both increases as we increase M and there is decreasing effect on momentum boundary layer for both Cases A and B. Fig(4.9-4.12) depicts the influence of Prandtl number on temperature and concentration profiles for both cases. Thermal boundary layer reduces and the concentration boundary layer exhibits overshoot near the sheet for higher values of Pr, though the concentration boundary layer thickness reduces. A minor variation (initially increasing near the sheet and then decreasing away from the sheet) is observed in the concentration boundary layer with the increase in the Prandtl number. The influence of Thermophoresis parameter and brownian parameter has been shown in Fig(4.13-4.20). The parameters Nt and Nb causes increment in thermal boundary layer for both Cases (A and B). The concentration profile increases with increase in parameter Nt while Nb parameter causes reduction for both Case A and Case B. The effect of Lewis number Le has been shown in Fig(4.21-4.22). It reduces the concentration profile for Case A and B. In Fig(4.23-4.25) the effect of viscosity variation parameter has been shown. It reduces momentum boundary layer while both the thermal and concentration layers becomes thick. The parameter ϵ causes

increment in thermal boundary layer as shown in Fig(4.26).

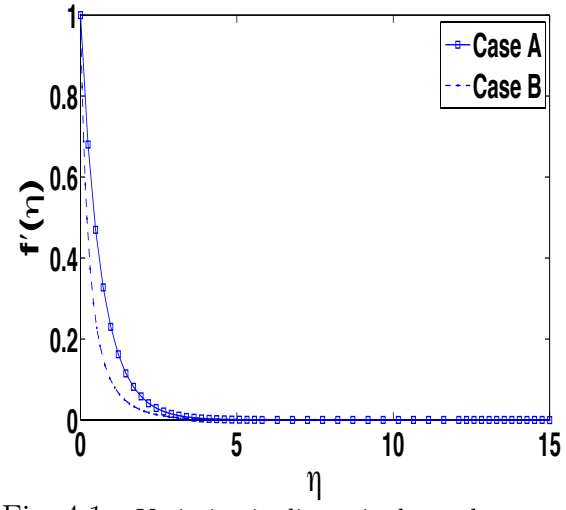

Fig. 4.1 – Variation in dimensionless velocity profiles $f'(\eta)$ for each Case A and B.

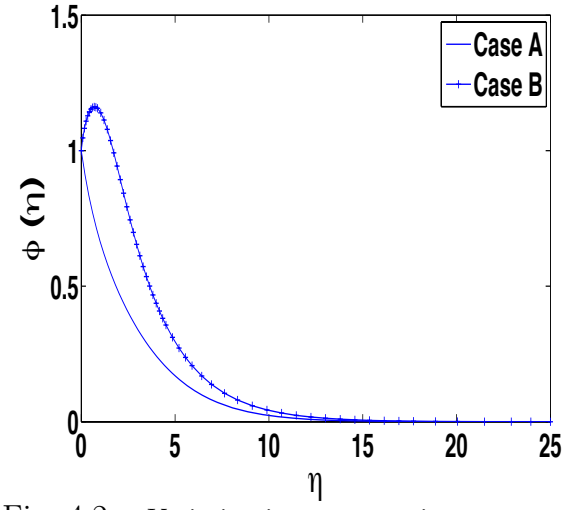

Fig. 4.2 – Variation in concentration profiles $\phi(\eta)$ for each Case A and B.

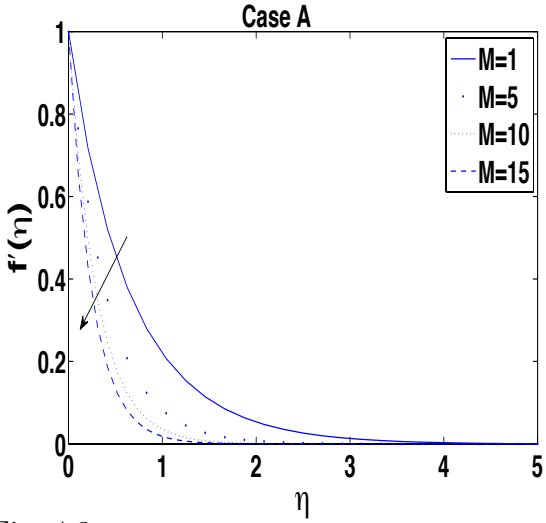

Fig. 4.3 – Variation in dimensionless velocity profiles $f'(\eta)$ for Case A.

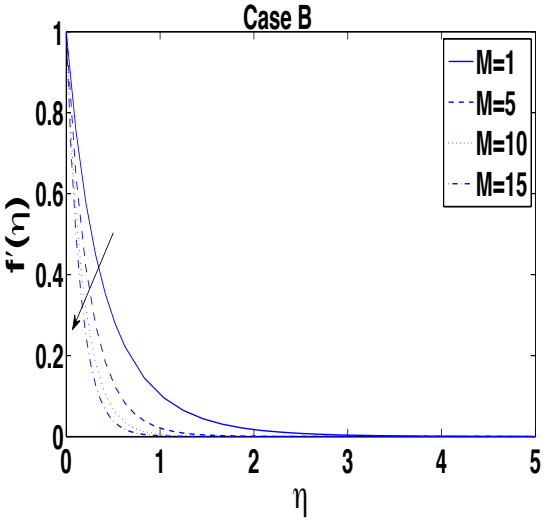

Fig. 4.4 – Variation in dimensionless velocity profiles $f'(\eta)$ for Case B.

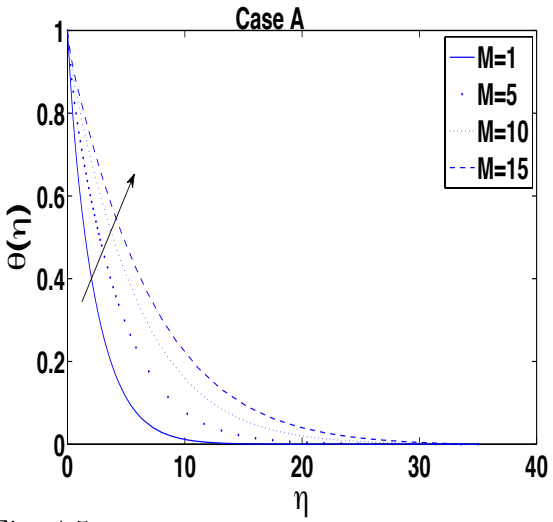

Fig. 4.5 – Variation in M and its impact on the dimensionless temperature profiles $\theta(\eta)$ for Case A.

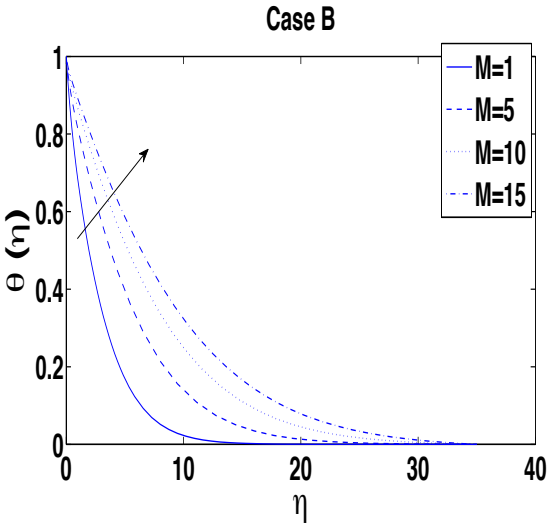

Fig. 4.6 – Variation in M and its impact on the dimensionless temperature profiles $\theta(\eta)$ for Case B.

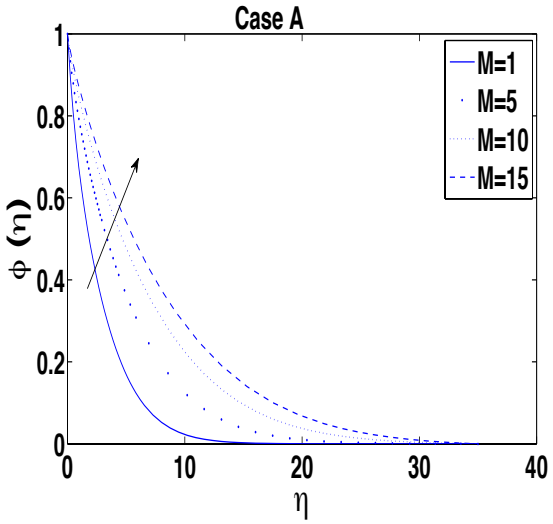

Fig. 4.7 – Variation in M and its impact on the dimensionless concentration profiles $\phi(\eta)$ for Case A.

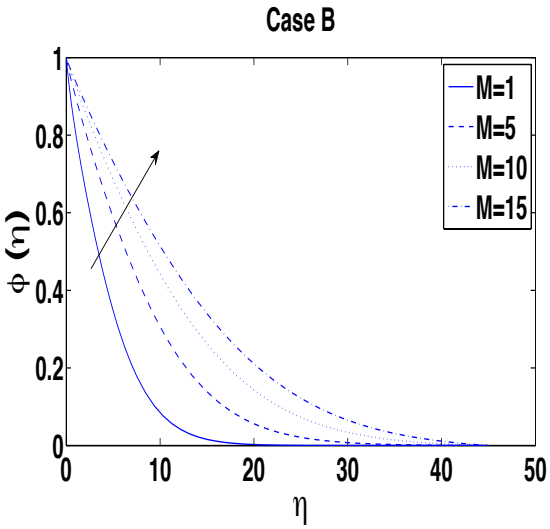

Fig. 4.8 – Variation in M and its impact on the dimensionless concentration profiles $\phi(\eta)$ for Case B.

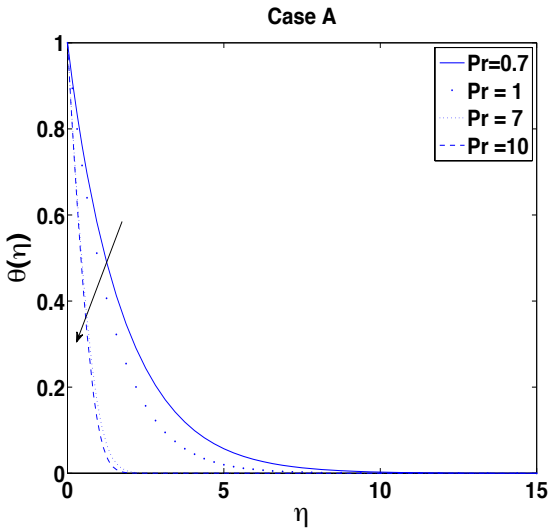

Fig. 4.9 – Variation in Pr and its impact on dimensionless temperature profiles $\theta(\eta)$ for Case A.

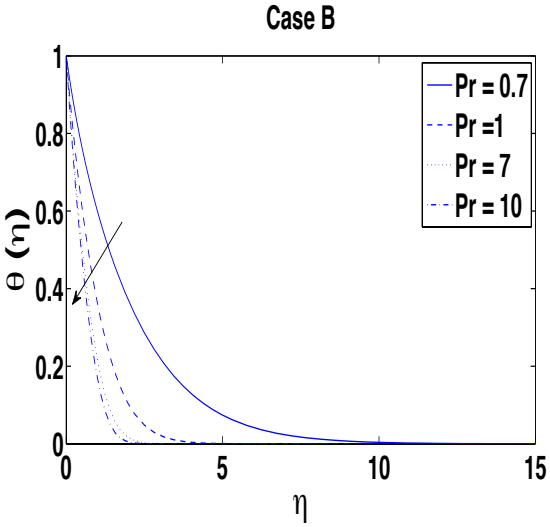

Fig. 4.10 – Variation in Pr and its impact on dimensionless temperature profiles $\theta(\eta)$ for Case B.

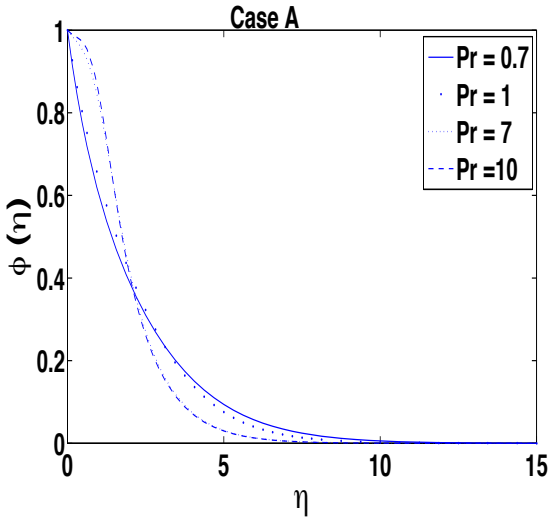

Fig. 4.11 – Variation in Pr and its impact on concentration profiles $\phi(\eta)$ for Case A.

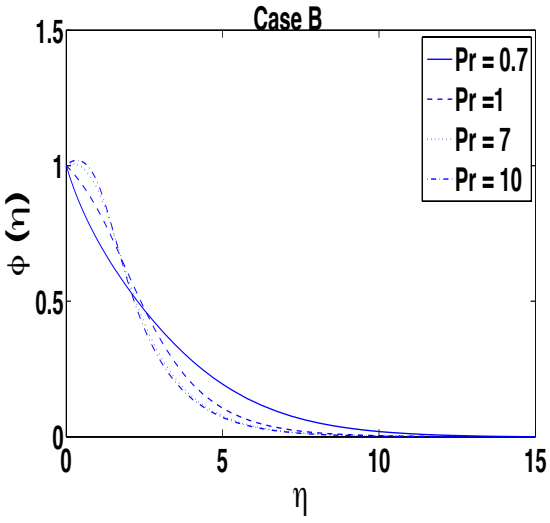

Fig. 4.12 – Variation in Pr and its impact on concentration profiles $\phi(\eta)$ for Case B.

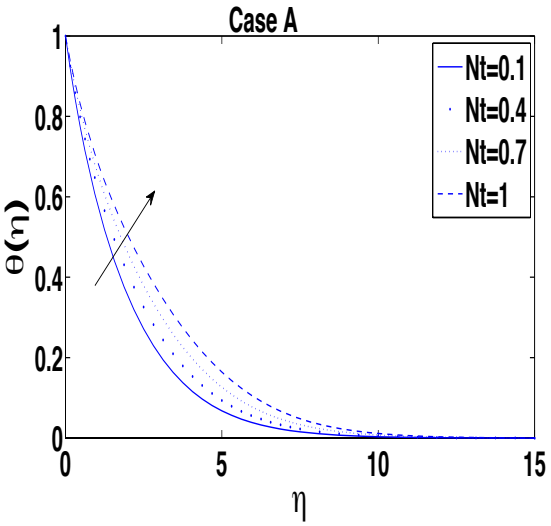

Fig. 4.13 – Temperature profiles $\theta(\eta)$ for various valus of Nt parameter.

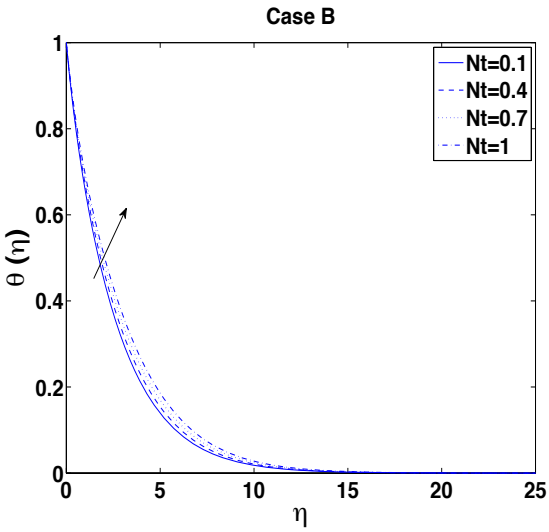

Fig. 4.14 – Temperature profiles $\theta(\eta)$ for various valus of Nt parameter.

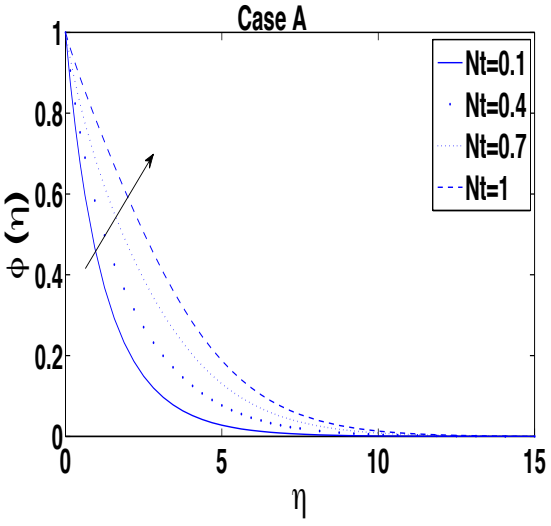

Fig. 4.15 – Variation in Nt and its impact on concentration profiles $\phi(\eta)$ for Case A.

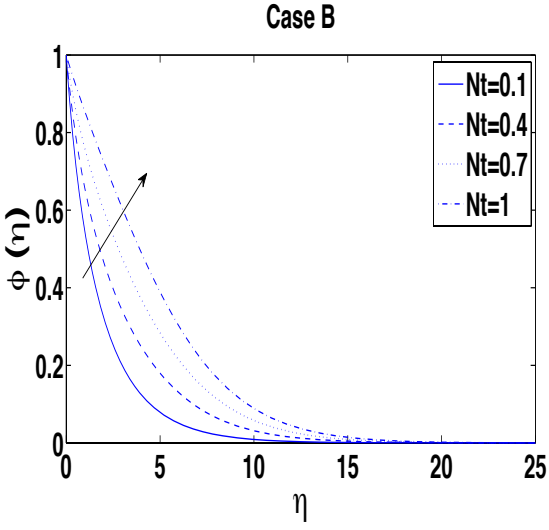

Fig. 4.16 – Variation in Nt and its impact on concentration profiles $\phi(\eta)$ for Case B.

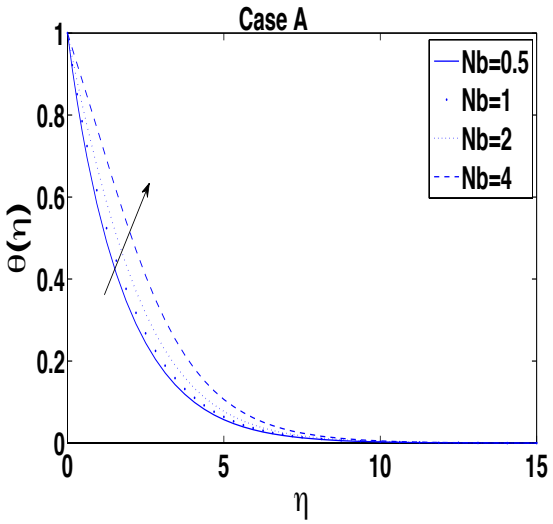

Fig. 4.17 – Variation in $\theta(\eta)$ for various values of Nb parameter.

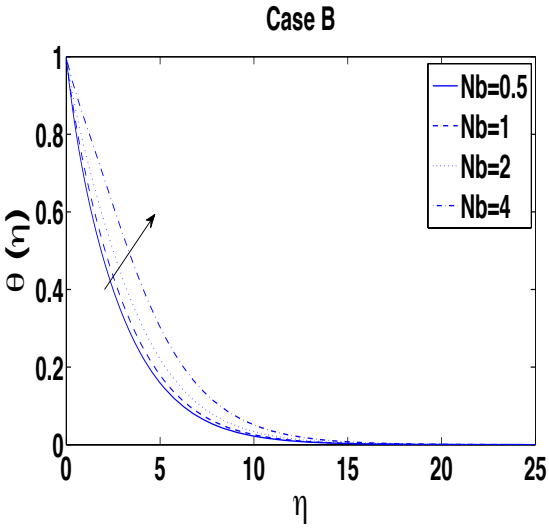

Fig. 4.18 – Variation in $\theta(\eta)$ for various values of Nb parameter.

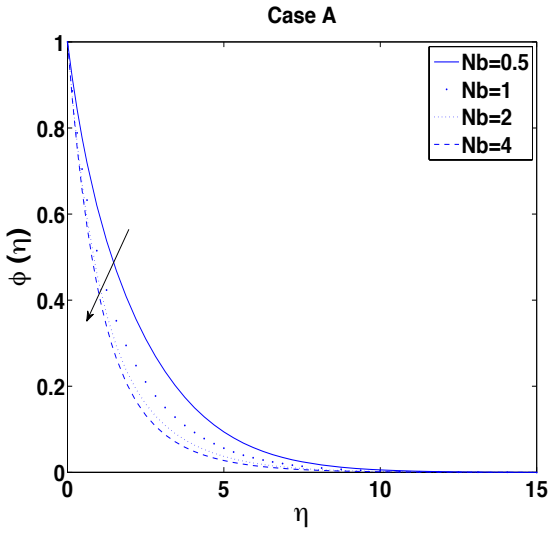

Fig. 4.19 – Variation in Nb and its impact on concentration profiles $\phi(\eta)$ for Case A.

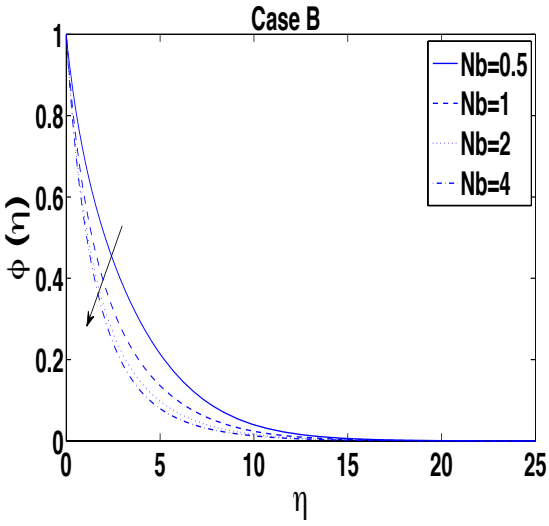

Fig. 4.20 – Variation in Nb and its impact on concentration profiles $\phi(\eta)$ for Case B.

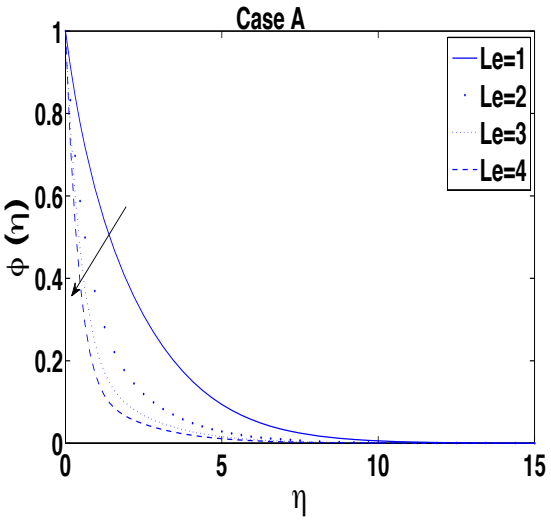

Fig. 4.21 – Variation in Le and its impact on concentration profiles $\phi(\eta)$ for Case A.

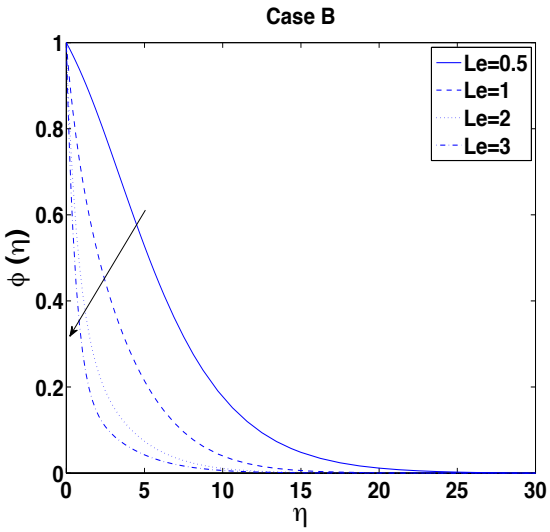

Fig. 4.22 – Variation in Le and its impact on concentration profiles $\phi(\eta)$ for Case B.

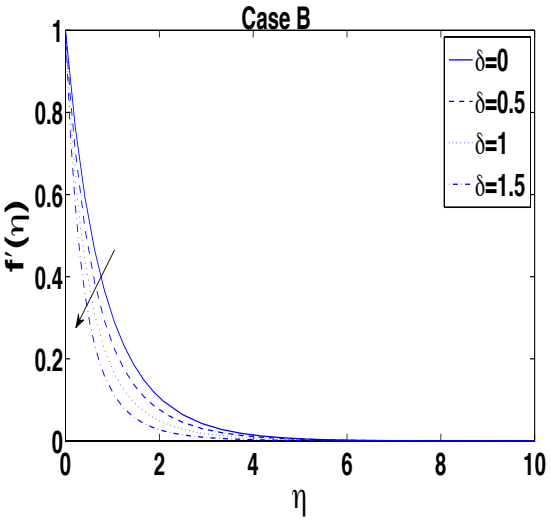

Fig. 4.23 – Variation in velocity profiles $f'(\eta)$ for various valus of δ parameter.

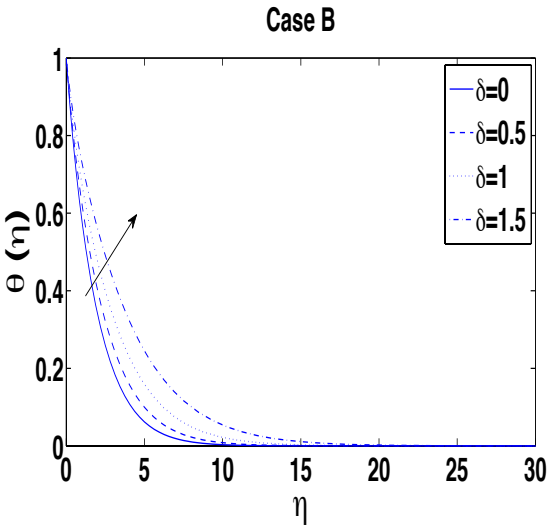

Fig. 4.24 – Variation in temperature profiles $\theta(\eta)$ for various valus of δ parameter

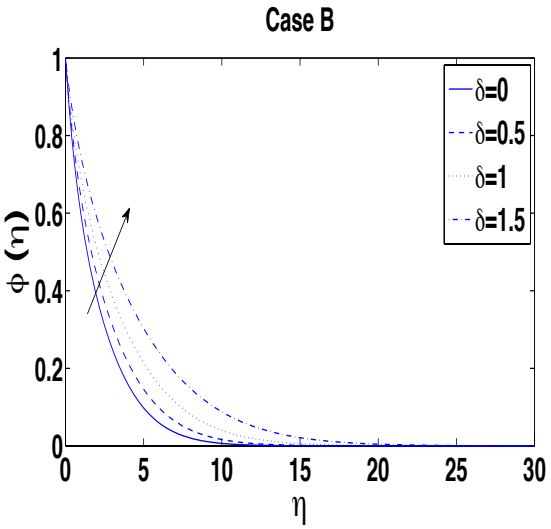

Fig. 4.25 – Variation in δ and its impact on the concentration profiles $\phi(\eta)$ Case B.

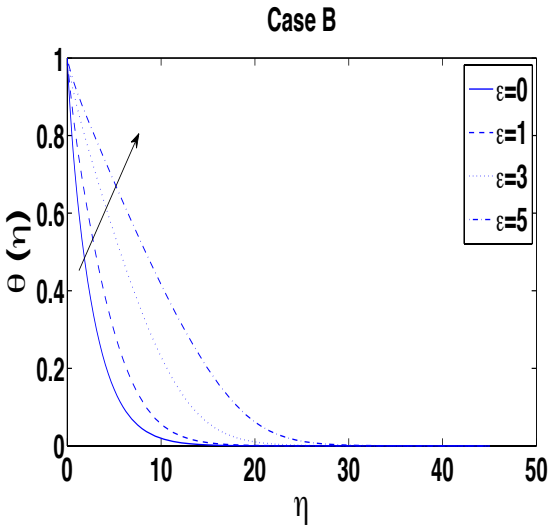

Fig. 4.26 – Variation in ϵ and its impact on temperature profiles $\theta(\eta)$ Case B.

4.8 Concluding Remarks

Skin friction coefficient and thermal boundary layer both increases with increment in magnetic parameter while velocity profile and wall temperature declines for both Case A and B. For both the cases Prandtl number causes thermal boundary layer to reduce whereas enhances momentum boundary layer. While it causes a slight change in skin friction and enhances wall temperature. Thermophoresis parameter causes both thermal and concentration boundary layer to increase for both Case A and B. It causes reduction in wall temperature. Skin friction reduces for Case B while for Case A it remains same. Brownian parameter increases thermal boundary layer while reduces concentration boundary layer and wall temperature for Case A and B. Skin friction for Case B reduces while for Case A it remians unaltered. For both Case A and Case B Lewis number reduces wall temperature and increases concentration gradient. Skin friction remains unchanged for Case A while for Case B it reduces.

Also it causes reduction in concentration boundary layer for both cases. Viscosity variation parameter reduces both wall temperature and concentration gradient while shows opposite behaviour for skin friction. Thermal and concentration boundary layer both increases while momentum boundary layer reduces as we increase δ. Parameter ϵ reduces both skin friction and wall temperature while concentration gradient and thermal boundary layer increases.

Chapter 5

Conclusion

In this chapter, we conclude all the results of previous chapters. In this dissertation, we studied MHD flow and heat transfer analysis of a viscous fluid over a nonlinearly and exponentially strecthing sheet. Comparison is made by taking constant and variable fluid properties. We have mainly focused on variable viscosity and thermal conductivity while keeping remaining properties as constant. Similarity transformation has been used to convert governing nonlinear PDEs into nonlinear ODEs. Resulting equations are solved numerically. The effect of different governing parameters such as magnetic parameter M, velocity exponent m, temperature index parameter n, stretching parameter β, brownian parameter Nb, viscosity parameter δ and the ϵ parameter on MHD flow and heat transfer are investigated. Various numerical results for skinn friction, local Nusselt number and local Sherwood number are obtained and are presented in tables. Velocity, temperature and concentration profiles are shown graphically. These computed results are also compared with previous literature.

Bibliography

[1] H. Blasius, Grenzschichten in flussigkeiten mit kleiner reibung, *Z. Angew. Math. Phys.*, (1908) 1-37.

[2] B. C. Sakiadis, Boundary-layer behavior on continuous solid surfaces: I. Boundary-layer equations for two-dimensional and axisymmetric flow, *AIChE.*, **7** (1961) 26-28.

[3] B. C. Sakiadis, Boundary-layer behavior on continuous solid surfaces: II. The boundary layer on a continuous flat surface, *AIChE.*, **7** (1961) 221-225.

[4] B. C. Sakiadis, Boundary-layer behavior on continuous solid surfaces: III. The boundary layer on a continuous cylindrical surface, *AIChE.*, **7** (1961) 467-472.

[5] V. M. Soundalgekar, T. V. Ramana Murty, Heat transfer in flow past a continuous moving plate with variable temperature, *Heat and Mass Transfer.,* **14** (1980) 91-93.

[6] A. Pantokratoras, Further results on the variable viscosity on flow and heat transfer to a continuous moving flat plate, *Int. J. Eng. Sci.*, **42** (2004) 1891-1896.

[7] H. Andersson and J. Aarseth, Sakiadis flow with variable fuid properties revisited, *Int. J. Eng. Sci.*, **45** (2007) 554-561.

[8] F. C. Lai and F. A. Kulacki, The effect of variable viscosity on convective heat transfer along a vertical surface in a saturated porous medium, *Int. J. Heat Mass Transfer.,* **33** (1990) 1028-1031.

[9] N. Bachok, A. Ishak and I. Pop, Boundary layer flow and heat transfer with variable fluid properties on a moving flat plate in a parallel free stream, *J. Appl. Math.*, **2012** (2012).

[10] T. C. Chiam, Magnetohydrodynamic heat transfer over a non-isothermal stretching sheet, *Acta Mech.*, **122** (1997) 169-179.

[11] S. Mukhopadhyay, G. C. Layek and S. k. A. Samad, Study of MHD boundary layer flow over a heated stretching sheet with variable viscosity, *Int. J. Heat Mass Transfer.*, **48** (2005) 4460-4466.

[12] I. Pop, R. S. R. Gorla and M. Rashidi, The effect of variable viscosity on flow and heat transfer to a continuous moving flat plate, *Int. J. Eng. Sci.*, **30** (1992) 1-6.

[13] K. V. Prasad, K. Vajravelu and P. S. Datti, The effects of variable fluid properties on the hydro-magnetic flow and heat transfer over a non-linearly stretching sheet, *Int. J. Thermal Sci.*, **49** (2010) 603-610.

[14] MA Seddeek, The effect of variable viscosity on hydromagnetic flow and heat transfer past a continuously moving porous boundary with radiation, *ICHMT.*, **27** (2000) 1037-1046.

[15] H. I. Andersson, MHD flow of a visco-elastic fluid past a stretching surface, *Acta Mech.*, **95** (1992) 227-230.

[16] K. B. Pavlov, Magnetohydrodynamic flow of an incompressible viscous fluid caused by deformation of a plane surface, *Magnitnaya Gidrodinamika (U.S.S.R.)*, **4** (1974) 146-147.

[17] MA Seddeek, Effects of radiation and variable viscosity on a MHD free convection flow past a semi-infinite flat plate with an aligned magnetic field in the case of unsteady flow, *Int. J. Heat Mass Transfer.*, **45** (2002) 931-935.

[18] E. M. A. Elbashbeshay and M. A. A. Bazid, The effect of temperature-dependent viscosity on heat transfer over a continuous moving surface, *J. Phys. D: Appl. Phys.*, **33** (2000) 2716-2721.

[19] J. X Ling and A. Dybbs, Forced convection over a flat plate submersed in a porous medium:variable viscosity case, *Am. Soc. Mech. Eng.*, **114** (1987) 87-123.

[20] M. Mustafa, Viscoelastic flow and heat transfer over a non-linearly stretching sheet: OHAM solution, *J. Appl. Fluid Mech.,* **9** (2016) 1321-1328.

[21] A. M. Jacobi, A scale analysis approach to the correlation of continuous moving sheet (backward boundary layer) forced convective heat transfer, *J. Heat Transfer.,* **115** (1993) 1058-1061.

[22] F. K. Tsou, E. M. Sparrow and R. J. Goldstein, Flow and heat transfer in the boundary layer on a continuous moving surface, *Int. J. Heat Mass Transfer.,* **10** (1967) 219-235.

[23] M. E. Ali, On thermal boundary layer on a power law stretching surface with suction or injection, *Int. J. Heat Mass Flow.,* **16** (1995) 280-290.

[24] L. F. Shampine, J. Kierzenka and M. W. Reichelt, Solving boundary value problems for ordinary differential equations in MATLAB with bvp4c, *Tutorial notes.,* **2000** (2000) 1-27.

[25] Bs Dandapat, Santra B, Vajravelu K, The effects of variable fluid properties and thermocapillarity on the flow of a thin flim on an unsteady stretching sheet, *Int. J. Heat Mass Transfer.*, **50** (2007) 991-996.

[26] Srinivas Maripala, Kishan Naikoti, Hall effects on unsteady MHD free convection flow over a stretching sheet with variable viscosity and viscous dissipation, *World Appl Sci J.*, **33** (2015) 1032-1041.

[27] PK Kameswaran, M Narayana, P Sibanda and G Makanda, On radiation effects on hydromagnetic Newtonian liquid flow due to an exponential stretching sheet, *Boundary Value Problems.*, **2012** (2012) 105.

[28] T. Hayat, Anum Shafiq and A. Alsaedi, MHD axisymmetric flow of third grade fluid by a stretching cylinder, *AEJ*, **54** (2015) 205-212.

[29] M. Jayachandra Babu, N. Sandeep, M. E. Ali and Abdullah O. Nuhait, Magnetohydrodynamic dissipative flow across the slendering stretching sheet with temperature dependent variable viscosity, *Results in physics.,* **7** (2017) 1801-1807.

[30] E. Magyari and B. Keller, Heat and mass transfer in the boundary layers on an exponentially stretching continuous surface, *J. Phys. D: Appl. Phys.,* **32** (1999) 577585.

[31] S. Nadeem, S. Zaheer and T. Fang, Effects of thermal radiation on the boundary layer flow of a Jeffrey fluid over an exponentially stretching surface, *Numerical Algorithms*, **57** (2011) 187-205.

[32] G. M. Pavithra and B. J. Gireesha, Effect of internal heat generation/absorption on dusty fluid flow over an exponentially stretching sheet with viscous dissipation, *Journal of Mathematics.*, **2013** (2013).

[33] Fazle Maboob, W. A. Khan and A. I. Md. Ismail, MHD flow over exponential radiating stretching sheet using homotopy analysis method, *JKSUS.*, **29** (2017) 68-74.

[34] R. L. V. Renuka Devi, T. Poornima, N. Bhaskar Reddy and S. Venkataramana, Radiation an Mass Transfer Effects on MHD Boundary Layer Flow due to an Exponentially Stretching Sheet with Heat Source, *IJEIT*, **3** (2014) 33-39.

[35] M. Subhas Abel, Mahantesh M, Nandeppanavar and Veena Basanagouda, Effects of Variable Viscosity, Buoyancy and Variable Thermal Conductivity on Mixed Convection Heat Transfer Due to an Exponentially Stretching Surface with Magnetic Field, *Proc. Natl. Acad. Sci. India Sect. A Phys. Sci.*, **87(2)** (2017) 247-256.

[36] F. M. White, Viscous Fluid Flow, third ed., McGraw-Hill, New York, (2006).

[37] D. Pal, Mixed convection heat transfer in the boundary layers on an exponentially stretching surface with magnetic field, *Applied Mathematics and Computation.*, **217** (2010) 2356-2369.

[38] Choi, S.U.S. and Eastman, J.A., Enhancing thermal conductivity of fluids with nanoparticles, (1995).

[39] W.A. Khan, O.D. Makinde, Z.H. Khan, Non-aligned MHD stagnation point flow of variable viscosity nanofluids past a stretching sheet with radiative heat, *Int. J. Heat Mass Transfer.*, **96** (2016) 525534.

[40] Tasawar Hayat, Muhammad Ijaz Khan, Muhammad Waqas, Tabassum Yasmeen, Ahmed Alsaedi, Viscous dissipation effect in flow of magnetonanofluid with variable properties, *Journal of Molecular Liquids.*, **222** (2016) 4754.

[41] J.Buongiorno, Convective transport in nanofluids, *Journal of heat transfer.*, **128** (2006) 240-250.

[42] M. Mustafa, M. Farooq, T. Hayat, A. Alsaedi, Numerical and Series Solutions for Stagnation-Point Flow of Nanofluid over an Exponentially Stretching Sheet, *PLOS ONE.*, **8** (2013).

[43] Shafaq Naz, Numerical Solutions of Boundary Layer Flows with Variable Fluid Properties, MS Thesis, National University of Sciences and Technology(NUST), 2016.